Time Dependent Rheological Response of Composite Binders

by

Aditya Inbasekaran

A Thesis Presented in Partial Fulfillment
of the Requirements for the Degree
Master of Science

Approved March 2016 by the
Graduate Supervisory Committee:

Narayanan Neithalath, Chair
Barzin Mobasher
Subramaniam Rajan

ARIZONA STATE UNIVERSITY

May 2016

ABSTRACT

The need for sustainability in construction has encouraged scientists to develop novel environmentally friendly materials. The use of supplementary cementitious materials was one such initiative which aided in enhancing the fresh and hardened concrete properties. This thesis aims to explore the understanding of the early age rheological properties of such cementitious systems.

The first phase of the work investigates the influence of supplementary cementitious materials (SCM) in combination with ordinary Portland cement (OPC) on the rheological properties of fresh paste with and without the effect of superplasticizers. Yield stress, plastic viscosity and storage modulus are the rheological parameters which were evaluated for all the design mixtures to fundamentally understand the synergistic effects of the SCM. A time-dependent study was conducted on these blends to explore the structure formation at various time intervals which explains the effect of hydration in conjecture to its physical stiffening. The second phase focuses on the rheological characterization of novel iron powder based binder system.

The results of this work indicate that the rheological characteristics of cementitious suspensions are complex, and strongly dependent on several key parameters including: the solid loading, inter-particle forces, shape of the particle, particle size distribution of the particles, and rheological nature of the media in which the particles are suspended. Chemical composition and reactivity of the material play an important role in the time-dependent rheological study.

A stress plateau method is utilized for the determination of rheological properties of concentrated suspensions, as it better predicts the apparent yield stress and is shown to

correlate well with other viscoelastic properties of the suspensions. Plastic viscosity is obtained by calculating the slope of the stress-strain rate curve of ramp down values of shear rates. In oscillatory stress measurements the plateau obtained within the linear visco-elastic region was considered to be the value for storage modulus.

Between the different types of fly ash, class F fly ash indicated a reduction in the rheological parameters as opposed to class C fly ash that is attributable to the enhanced ettringite formation in the latter. Use of superplasticizer led to a huge influence on yield stress and storage modulus of the paste due to the steric hindrance effect.

In the study of iron based binder systems, metakaolin had comparatively higher influence than fly ash on the rheology due to its tendency to agglomerate as opposed to the ball bearing effect observed in the latter. Iron increment above 60% resulted in a decrease in all the parameters of rheology discussed in this thesis. In the OPC-iron binder, the iron behaved as reinforcements yielding higher yield stress and plastic viscosity.

ACKNOWLEDGMENTS

I would like to sincerely thank everyone who has contributed and helped me throughout my thesis. First and foremost, I wish to thank my advisor Dr. Narayanan Neithalath for showing faith in me and giving me the opportunity to work in his research group. Your guidance through this process; discussions, ideas, and feedback have been invaluable.

I would also like to thank my committee members Dr. Barzin Mobasher and Dr. Subramaniam Rajan for providing their feedback and guidance. I would also like to express my gratitude to all my fellow researchers in the group who have contributed to this thesis directly or indirectly.

It would not be sufficient enough to just thank my room-mate and mentor in research Akash Dakhane for his support over the last two years. I will always be grateful from the bottom of my heart for this. I would also like to thank Akshay Gundla, Aashay Arora, Dr. Sumanta Das and Dr. Ahmet Kizilkanat for their technical guidance in the subject. I would also like to acknowledge Namrata and Omkar, my best friends who helped along the way.

Finally, I would like to thank and dedicate this thesis to my Mom and Dad. I am grateful to you for believing in my dreams to make my wishes come true. I can only imagine the sacrifices you both have made to make me the man I am today. Everything that I could achieve today wouldn't be possible without you both.

TABLE OF CONTENTS

Page

CHAPTER Page

CHAPTER Page

LIST OF TABLES

LIST OF FIGURES

Figure Page

1 INTRODUCTION

In recent years, there has been a growing importance to develop and understand environment friendly materials. Concrete is the second most used material in the world after water. The manufacturing process for cement, the binding constituent in concrete, produces enormous amounts of carbon dioxide. CO_2 is a green-house gas and contributes to global warming, therefore researchers have tried to come up with alternate filler materials which could partially replace cement in concrete. There have been a number of studies on replacement of cement with supplementary cementitious materials (SCMs) such as class F fly ash, class C fly ash, ground granulated blast furnace slag, metakaolin and inert fillers such as limestone. Class F fly ash is a by-product of combustion of anthracite and bituminous coal in thermal power plants, whereas class C fly ash is obtained from burning younger lignite or sub-bituminous coal.

These SCMs have been shown to replace OPC by 10% to 50% depending on the type of SCM used. Studies confirm that all these SCMs contribute to the strength of concrete, it also densifies the microstructure and reduces the permeability (Dhir and Jones 1999). Other benefits are freeze-thaw resistance, sulfate resistance, soundness etc. Limestone can replace OPC by up to 15% by mass which is a filler material and shows its particle size effects on hydration and strength (Arora, Sant, and Neithalath 2016). Apart from advantages to hardened cement, SCMs also have proven to be advantageous to fresh cement properties like workability, heat of hydration, setting time, shrinkage cracking etc. (Brooks and Megat Johari 2001; Siddique and Klaus 2009; Frías, de Rojas, and Cabrera 2000)Earlier studies have accounted for a time dependent study of fresh cement paste or

rheology of SCMs immediately after mixing.

As a part of the current study, a detailed study was conducted to understand the rheological properties of cement pastes partially replaced by class C or class F fly ash over a period of two hours. In addition to this, another series of experiments were conducted on ternary blends of OPC containing class F fly ash and limestone and the effect of super plasticizer on the rheological properties of these blends was investigated. The various parameters were evaluated using a rheometer and the reaction kinetics were characterized using isothermal calorimetry. The experimental results were corroborated by computational simulations to elucidate the influence of contact fraction, specific surface area and volume of solids. The study gives an insight into which proportion of these blends would be appropriate for different scenarios thus enabling new techniques to proportion binders. This was a time dependent study and therefore it carefully explains the hardening of the paste over the span of two hours from the time of mixing.

Another study in this dissertation was the rheological evaluation of a novel material based on the iron powder binder system for purpose of application in the industry.

1.1 Objectives

The main objectives of this study are as follows:

i. Yield stress, plastic viscosity and storage modulus have been evaluated for different binary and ternary blends along with super-plasticizer and compared to plain OPC to find the advantages and disadvantages of these blends as compared to conventional OPC.

ii. The same parameters were obtained for novel binding material containing a blend of iron powder, class F fly ash, limestone, metakaolin and oxalic acid. The method

of preparation for this material differs from the conventional method of fabrication, however it is beneficial to evaluate the rheology of a material that could be a potential replacement to OPC in construction.

1.2 Thesis Layout

Chapter 2 provides a literature review of past studies on rheology of OPC. It includes time-dependent study of various parameters of OPC and the rheology of supplementary cementitious materials. A brief study on the iron powder based binder system has been provided. Different techniques to perform rheological experiments have also been reviewed.

Chapter 3 details the experimental design, including raw material properties, mixture proportions, mixing procedures and test methods used to assess the properties of the blended binder systems.

Chapter 4 discusses the findings of the rheological studies in binary and ternary blends of cement. A time dependent comparison of parameters like plastic viscosity, yield stress, storage modulus is brought out in this chapter and reasonable explanations with respect to particle shape and contact fraction are used to corroborate the experimental results.

Chapter 5 is devoted to understanding the rheology of novel iron based binder and corresponding scientific explanations are provided to support the findings.

Chapter 6 provides a detailed conclusion of the rheological studies carried out on the supplementary cementitious materials.

2 LITERATURE REVIEW

This chapter discusses the previous research conducted on ordinary Portland cement, supplementary cementitious materials and rheology of these materials.

2.1 Background and Overview

Ordinary Portland cement concrete (OPCC) is being used in construction for more than a hundred years. It is the most widely used resource in the world after water and hence poses a direct impact on the world economy and environment. OPC is a cheap construction material, but its extensive has some impact on the economy. It has a huge impact on environmental pollution because it produces huge amount of carbon dioxide.

The manufacturing process of OPC involves excessive production of carbon dioxide and this contributes to 5% of global anthropogenic CO_2 (Worrell et al. 2001; Hendriks et al. 2002). OPC manufacturing process involves heating of raw materials like silica and limestone at very high temperature of about 1500˚C inside the kiln. The production of such heat uses energy of up to 5 MJ/ton (Government of Canada 2009). Hence there was a need for a sustainable substitutive material for OPC, which is being researched by the use of supplementary cementitious materials. These SCMs can either be pozzolanic i.e. alumino-silicates or just inert fillers like limestone.

Fly ash is a by-product of the combustion of pulverized coal in thermal power plants and is highly pozzolanic. The chemical composition of fly ashes depends on the characteristics and composition of the coal burned in power stations. The chemical analysis of fly ashes by means of X-ray fluorescence (XRF) and spectrometry techniques shows that SiO_2, Al_2O_3, Fe_2O_3, and CaO are the major constituents of most fly ashes. Other elements are MgO, Na_2O, K_2O, SO_3, MnO, TiO_2, and C. As mentioned earlier, based on the type of coal

there are two types of fly ash: class C and class F. Other SCMs are obtained from similar processes. They react with calcium hydroxide (CH) formed from the hydration of OPC to further form C-S-H gel which adds to the strength of the paste. The quantity and composition of the C-S-H gel are greatly affected by the type and amount of SCM. The addition of an appropriate amount of an SCM leads to the formation of C-S-H gel with a low Ca/Si ratio, resulting in lower concentrations of alkali and hydroxide ion in the pore solution, which is the most effective factor for alumino silicate reation (ASR) suppression. In order to evaluate the suppression effect of SCMs on ASR expansion, it is necessary to consider the hydration process of cement and SCMs as well as the properties of the cement hydrates. There is excess cement in the paste which is left unhydrated and hence remains unused, in this case limestone is used to partially replace OPC to avoid wastage of material and bring down the cost of construction.

These SCMs not only make the concrete environmental friendly but also have other advantages and disadvantages. Addition of SCMs to OPC improves the chemical and mechanical properties of concrete. In depth studies have found advantages of fly ash as a replacement to OPC at later ages. It improves the durability, reduces shrinkage, etc. which will be explained in the following section. Also they have improved the early age properties like workability, pumpability, setting time, etc. Some critical rheological properties like yield stress, plastic viscosity, storage modulus are studied in depth in this thesis over a period of 2 hours from the time of mixing which will be substantiated by 3D simulations yielding particle contact fractions.

Also another system containing metakaolin, fly ash, limestone, iron powder and oxalic acid which was tested for later age properties such as compressive strength and flexural

strength, yielded enhanced results (Das et al. 2014). This system was also evaluated for rheological studies in this thesis to understand the flowability of the material for it to be placed in the formwork.

Final study was carried out on OPC replaced by iron powder which act as reinforcement to provide enhanced tensile toughness and yield improved fracture resistant properties (Das, Kizilkanat, and Neithalath 2015). The rheological parameters of this system were also studied as a part of this thesis.

2.2 Significance of Ordinary Portland cement.

Ordinary Portland cement is one of the major constituents in concrete and has a wide variety of uses. Nowadays OPC is manufactured by a dry process in which limestone and clay are crushed and mixed with water to form a slurry. This slurry passes through a kiln at temperature of about 1500˚C which changes the raw mix chemically into cement clinker. At the end of the process gypsum is added to clinker to avoid flash set. The various reactions such as calcination and clinkering reaction give rise to clinker which is then ground to fine powder. There are different phases present in OPC, namely C_3S, C_2S, C_3A and C_4AF.

2.2.1 Physical and Chemical Properties.

Fineness, or particle size of ordinary Portland cement affects rate of hydration, which influences the rate of strength gain. The smaller the particle size, the greater the surface area-to-volume ratio, which will lead to more area available for water-cement reaction per unit volume. Approximately 95% of cement particles are smaller than 45 micron with the average particle size about 15 micron. Fineness is measured in terms of surface area per unit mass and measured using Blaine's air permeability test or particle size analyzer.

The density of OPC is 3.15 g/cc which is found using Le Chatelier apparatus. Composition of OPC constituents is as shown in Table 1.

Table 1: Chemical Composition of Ordinary Portland Cement (OPC) used in this Study.

Constituent	CaO	SiO_2	Al_2O_3	Fe_2O_3	MgO	Alkalis	Sulfates
Percentage (%)	63.75	21.06	3.86	3.55	1.83	0.6	2.93

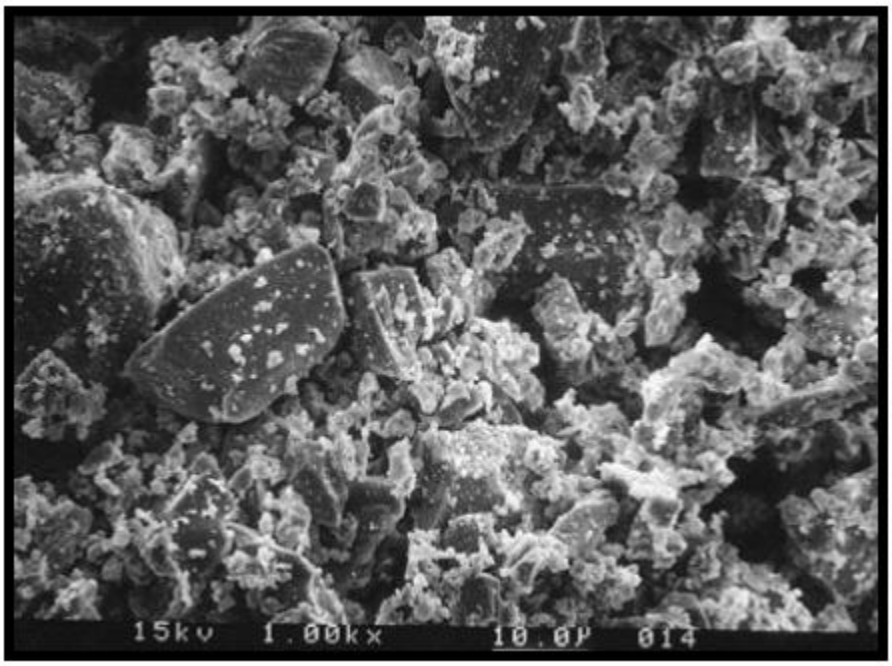

Figure 1: SEM Image of Ordinary Portland Cement. The Scale Bar Corresponds to 10 micron.

An image of the microscopic OPC particles surrounded by its hydration products as seen from a scanning electron microscope are shown in Figure 1. The OPC particles are highly angular in shape which impart viscosity to the material in a fresh state after mixing.

2.2.2 Reaction Kinetics

OPC gains strength by a process called hydration and during this, there is an evolution of thermal energy also called as heat of hydration due to exothermic reaction. C_3S and C_2S in

cement combine with water to form C-S-H and CH which produces 173.6 kJ and 58.6 kJ of heat respectively as found by isothermal calorimetry results. Figure 2 shows a representative curve of heat evolution of OPC when mixed with water.

$$2\ C_3S + 11\ H \rightarrow 3\ C\text{-}S\text{-}H + 3\ CH\ (+173.6\ kJ)$$

$$2\ C_2S + 9\ H \rightarrow 3\ C\text{-}S\text{-}H + CH\ (+58.6\ kJ)$$

$$3C3A + 3\ Gypsum + 26\ H \rightarrow 6\ (Ettringite)$$

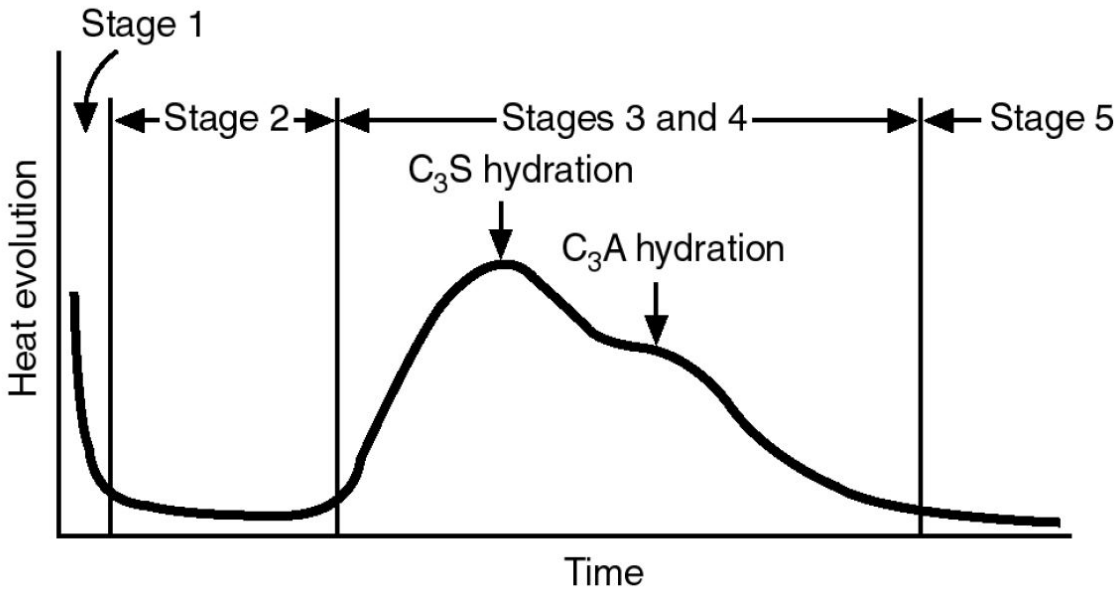

Figure 2: Heat Evolution Curve of OPC Obtained from Isothermal Calorimetry.

CH is water soluble and thus is a weak link in cement and concrete from a durability point of view. If the paste is exposed to fresh water, the CH will leach out (dissolve), increasing the porosity and thus making the paste more vulnerable to further leaching and chemical attack. C_3A reacts with gypsum and water to form ettringite which are needle shaped particles, which further reacts with C_3A again to form mono-sulfoaluminate. C_3A also forms tetra-calcium aluminate hydrate by reacting with CH.

C_3S and C_3A are responsible for early age strength development and produce high heat as

can be seen from Figure 2. C_2S imparts slow strength gain in the material over a period of days and the grey color of the cement is an attribute of C_4AF. Gypsum as mentioned above is added to avoid flash set of the material. The mineral composition of OPC used in this study is tabulated in Table 2.

Table 2: Concentration of Different Components of OPC.

Name	C_3S	C_2S	C_3A	C_4AF	Gypsum
Weight %	55	19	10	7	4

The timeline for the formation of products during the hydration of OPC is depicted in Figure 3. It is observed that with increase in product formation there is a decrease in the porosity of cement. Cement gains more than 90% of its strength in a period of 28 days but the process of hydration may continue for an even prolonged time with its rate of strength gain reducing with time.

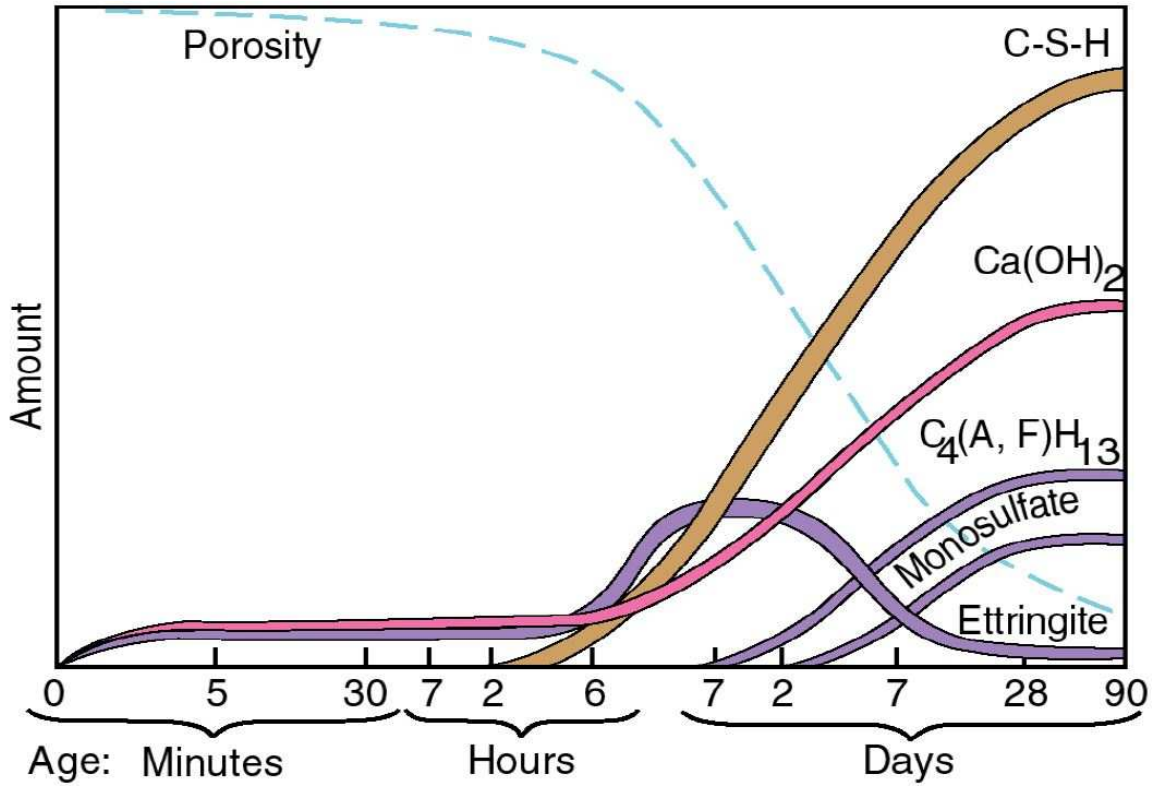

Figure 3: Formation of Hydration Products as a Function of Time.

2.2.3 Properties of Fresh and Hardened Cement Paste.

Any solid composed of randomly arranged particles, is both porous and permeable. Since cement paste has such structure, it is intrinsically porous and permeable. The completely hydrated cement paste has a porosity between 5% to 26% (Röβler and Odler 1985). The porosity of paste depends on the initial water content and on the extent to which the voids can be filled with hydration products. It depends, therefore, on the initial water-cement ratio and on the curing conditions. These pores allow the permeability of reactive ions which lead to sulfate attack and corrosion of the steel bars in the concrete, to prevent this, admixtures or pozzolans are used as an addition or replacement to OPC for enhanced particle packing. Porosity of hardened OPC is evaluated using mercury intrusion porosimetry (MIP).

As indicated, cement gel is regarded as a solid substance having a characteristic relatively high porosity with a pore size range of 0.05 to 10 microns. From the assumption that this substance has intrinsic strength depending on its composition and structure, and that the strength of the gel is the sole source of the strength of hardened paste. It follows that the strength of a specimen of paste should he related to the amount of gel within its boundaries. Furthermore, an assumption that the relative strength of the paste depends on the degree to which gel fills the pores available to it, leads to the establishment of an empirical relationship between the porosity and the strength of a paste (Powers 1958).

Soundness refers to the ability of a hardened cement paste to retain its volume after setting. Lack of soundness is observed in the cement samples containing excessive amounts of hard-burnt free lime or magnesia. Autoclave expansion test is used to determine soundness of cement.

Early age properties of OPC are also equally important which makes the concrete workable. Earlier studies found that parameters like yield stress and plastic viscosity are attributed to particle size, PSD's, contact fraction and distance between particles (Voigt et al. 2005).

2.3 Supplementary Cementitious Materials (SCMs).

In the last few decades the concept of sustainable construction has gained momentum and thus OPC has been partially replaced by other environmentally safe materials like SCM. There are a variety of SCMs i.e. class F fly ash, class C fly ash, slag, silica fume, metakaolin etc. All these materials impart variable properties to the concrete depending on its particle size, composition and reactivity.

2.3.1 Physical Properties.

The particle size of SCMs ranges within a wide spectra and the mean particle size is often smaller than OPC. The mean particle size of fly ash, silica fume, metakaolin are between 1 to 100 micron, 1 micron and 2 micron respectively. Limestone is manufactured under controlled conditions and therefore, its size can be obtained as required. Table 3 describes the fineness, specific gravity and figure 4 shows the different SCMs. The particle size distribution of all these materials are shown and discussed in detail in chapters 4 and 5.

Figure 4: Different Types of SCMs.

Table 3: Fineness and Specific Gravity of SCMs.

Material	Fineness (m^2/kg)	Specific gravity (g/cc)
Fly ash	400-700	1.9-2.8
Slag	400-600	2.85-3
Silica fume	20000	2.2-2.5
Metakaolin	19000	2.5

Table 4: Chemical Composition of Various SCM.

(%)	Class F fly ash	Class C fly ash	Slag	Silica fume	Metakaolin
SiO_2	52	35	35	90	53
Al_2O_3	23	18	12	0.4	43
Fe_2O_3	11	6	1	0.4	0.5
CaO	5	21	40	1.6	0.1
SO_3	0.8	4.1	9	0.4	0.1
Na_2O	1	5.8	0.3	0.5	0.05
K_2O	2	0.7	0.4	2.2	0.4
Total Na eq. alkali	2.2	6.3	0.6	1.9	0.3

Chemical composition of SCMs have been shown in Table 4. The shape of these particles

also play an important role in influencing the early age properties. Fly ash and silica fume are spherical in shape whereas slag and metakaolin have plate like particles. Images of these particles as seen through the SEM are shown in Figure 5.

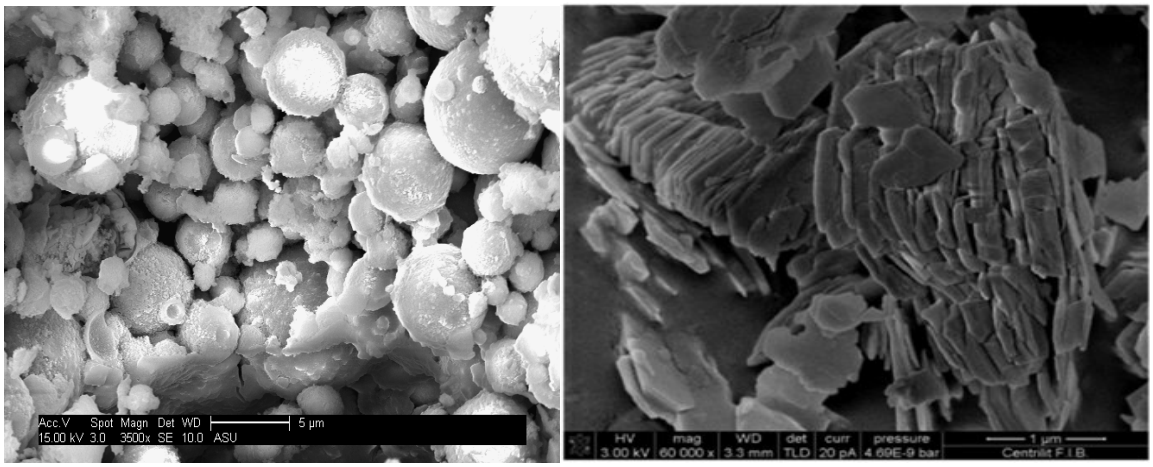

Figure 5: SEM Image of a) Fly ash b) Metakaolin.

2.3.2 Hardened Cement Properties.

First we shall discuss the effects of the SCMs on later age properties of cement. All SCMs contribute to the strength of concrete, depending on whether it has been used as a replacement or as an addition. When SCM is used as a cement replacement, strength development may be slower than when used as an addition. Most SCMs are pozzolans i.e. contain alumino silicates species, which react with the calcium hydroxide (CH) formed during hydration of OPC to produce more C-S-H gel which adds to strength development.

$$\text{Pozzolans} + \text{CH} \rightarrow \text{C-S-H}$$

This reaction is called the pozzolanic reaction and makes the concrete denser, water soluble CH is converted to strength and stability inducing C-S-H. A highly densified system means less air voids, thus use of SCM have reduced permeability and adsorption which indirectly has enable the concrete to be resistant to sulfate attack , corrosion and chemical attacks etc.

Hence the use of SCMs positively impacted the strength and durability characteristics. Limestone is an inert material and mainly plays an important role in early and later age properties only due to its particle size. Finer particles provide better packing density of the microstructure whereas coarse particles make the concrete relatively more porous.

2.4 Metallic Iron powder.

For the first time, the possibility of carbonating waste metallic iron powder to develop sustainable binder systems for concrete was explored by Sumanta (Das et al. 2014).

The fundamental concept behind using metallic iron powder is that it reacts with aqueous CO_2 under controlled conditions to form complex iron carbonates which have binding capabilities. Additives like fly ash and metakaolin were added to facilitate iron dissolution and to obtain beneficial rheological and later age properties. The influence of these materials on the rheological parameters of the binder system is the premise of the chapter 4 of this thesis. In another study of metallic powder, Sumanta replaced OPC by iron powder up to 30 % to study the fracture response of composite mortars. The research revealed an increase in strain energy release rate and increase in fracture process zone. Chapter 4 of this thesis also discusses the rheology of this OPC-iron binder system with the help of various rheological parameters such as yield stress, plastic viscosity and storage modulus.

2.5 Rheology.

Rheology is the study of flow in any material, typically fluids (Barnes 2000). This study is usually carried out by applying a controlled strain or stress for both linear and oscillatory rheometry; and the response of the material is measured. Research on flow of various materials have been carried out, including investigations into food processing (Bayod, Willers, and Tornberg 2008; Steffe 1996), blood (Cerny, Cook, and Walker 1962; Dintenfass

1976), and construction materials such as asphalt (Chomton and Valyer 1972; Gaskins et al. 1960) and concrete (Banfill 2003). The investigation of rheological properties of cementitious materials is very important, as it assists and aids in the casting, pumping and finishing of concrete structures.

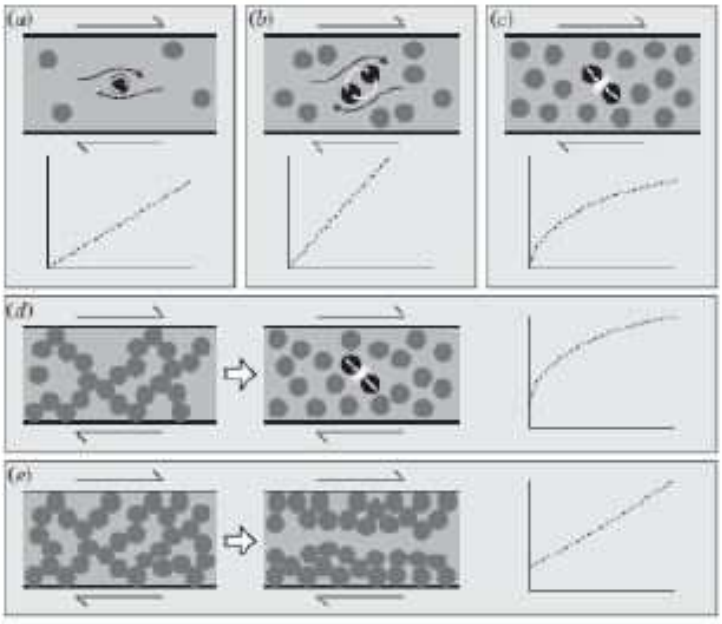

Figure 6: Graphical Depiction of the Influence of Solid Loading on the Flow Behavior of Suspensions (Mueller, Llewellin, and Mader 2009)

An in depth study of these materials shows that physico-chemical interactions, particle shape, solid loading, particle size of the suspended species and the suspension itself influences the rheology of the paste. Particle interaction involves effects such as particle contact forces, electrostatic forces, and van der Waals forces. The DLVO theory (named for Derjaguin, Landau, Verwey, and Overbeek) explains the colloidal stability and the behavior of colloidal suspensions through electrostatic repulsive forces and attractive van der Waals forces respectively. The influence of solid loading on the rheological behavior of suspensions has been rigorously studied for various suspensions; a typical depiction of this effect is presented

in Figure 6 (Mueller, Llewellin, and Mader 2009). At very low volume fraction the behavior of the material is seen to be Newtonian with linear flow curve and zero stress intercept. As the solid loading rises, shear thinning behavior is observed by formation of curvature in the figure, still a zero stress intercept prevails. Shear thinning occurs due to counter motion called the Brownian motion which tries to restore the original particle configuration that has been disturbed due to applied shear stress. Further solid loading causes high particle interaction and forms networks between particles that induces a non-zero stress intercept called the apparent yield stress.

Rotational rheology of concentrated suspensions are commonly divided into two types, linear shear rate response and oscillatory shear studies. The linear shear rate investigates the apparent yield stress and plastic viscosity from the flow curves. These parameters are extracted using various models like Bingham (Bingham 1922), Casson (Casson 1959), and Herschel-Bulkley (Herschel and Bulkley 1926).

$$\text{Bingham: } \tau = \tau_y + \eta_p \dot{\gamma}$$

$$\text{Herschel–Bulkley: } \tau = \tau_y + K\dot{\gamma}^{n}$$

$$\text{Casson: } \sqrt{\tau_y} + \sqrt{\eta_\infty}\sqrt{\dot{\gamma}}$$

The use of the Bingham model in the shear rate range (5-100/s) is justified by the generally linear nature of the shear stress–shear rate response. The rheological parameters for the 'wide' shear rate range (0.005–100/s) were calculated using a least squares fitting of the down-ramp data to two different models, sometimes referred to as generalized Bingham models: i.e. the Herschel–Bulkley model and the Casson model. The latter models were used because of their ability to better capture non-linearities in the data that manifests at lower shear rates. In these equations, τ is the shear stress (in Pa), τ_y is the yield stress (in

Pa), η_p is the plastic viscosity (in Pa s), $\dot{\gamma}$ is the shear rate (in s^{-1}), K is the consistency index which is a measure of the average viscosity of the fluid, and n is the flow behavior index, which ranges between 0-and-1 for shear thinning suspensions, and η_∞ (in Pa s) is the viscosity at an infinite shear rate (Vance, Sant, and Neithalath 2015).

Oscillatory shear experiments are conducted at low strains and used to explore the visco-elastic properties viz. storage modulus and loss modulus of the suspensions (Barnes 2000). When a linear viscoelastic body is subjected to stress varying sinusoidally with time at a certain frequency, the corresponding strain is not in the same phase as applied stress, which results in a phase lag between strain and stress as shown in Figure 7. The applied stress can be separated into two independent components: one is exactly in phase with strain, the other is $\pi/2$ out of phase as shown in Figure 7(b) (Sun, Voigt, and Shah 2006).

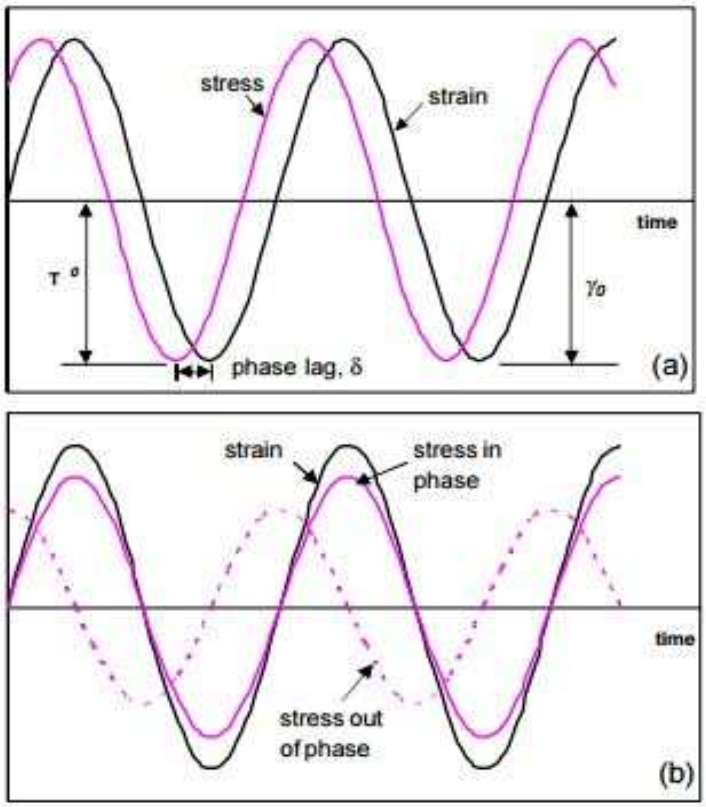

Figure 7: Stress and Strain Relation in a Viscoelastic Material (Mason 1949).

The relationship between stress and strain of a viscoelastic material can be established by using the modulus of rigidity in a complex format. If a material is subjected to a shear deformation, the shear modulus can be expressed as follows,

$$G^* = \frac{\tau}{\gamma} = G' + iG''$$

$$G' = \frac{\tau}{\gamma}\cos\delta$$

$$G'' = \frac{\tau}{\gamma}\sin\delta$$

where G* is the complex shear modulus, G' is the storage shear modulus, which represents the elastic behavior or the energy storage of the material, and G" is the loss shear modulus, which represents the viscous behavior or energy dissipation of the material. The phase lag

(δ) between stress and strain, which changes between 0 and π/2 can also be used to describe the material behavior. When a material is ideally elastic, the phase lag (δ) equals to zero; when a material is ideally viscous, parameter δ equals to π/2 (Sun, Voigt, and Shah 2006).

2.6 Rheology and Flow of Fresh Cement and Concrete

The flow of concrete on the field is tested by the slump cone test ("ASTM C143 - 12. Standard Test Method for Slump of Hydraulic-Cement Concrete" 2012). Concrete is poured into the cone shaped mold and the mold is taken off allowing the concrete to spread, the diameter to which it spreads determines the flowability and is often taken to be a measure of yield stress (Saak, Jennings, and Shah 2001; Roussel 2006; Roussel and Coussot 2005). This technique does not produce consistent results, this is because a single parameter cannot effectively model the flow of concrete and thus the yield stress measurements are not reliable.

An improved method of testing Portland cement suspensions in the laboratory is through use of viscometers or rheometers. Many studies involve experiments on cement pastes, rather than of the concrete, and relate the properties of the paste to the properties of concrete (Banfill 2003). This is because there are no rheological instruments yet, to measure the rheological characteristics of concrete. In concrete, sand and aggregates are the suspension and the suspending fluid is the paste, while the paste itself has Portland cement, gypsum and hydration products as suspensions in water. This complex system is thus difficult to study. Some studies have developed large scale viscometers to perform these types of investigations; however, the focus here will be on the rheological characterization of cementitious pastes.

Several past reviews have been documented on rheology of cementitious materials, one such comprehensive study was conducted by Banfill which has complete discussion of the topic (Banfill 2006).

In general rheological studies have been focused on two key areas: the influence of cement constitution on the rheological performance of cementitious suspensions (Park, Noh, and Park 2005; Bentz et al. 2012; Grzeszczyk and Lipowski 1997; Ferraris, Obla, and Hill 2001) and the influence of admixtures on these suspensions (Burgos-Montes et al. 2012; Asaga and Roy 1980; Gołaszewski and Szwabowski 2004; Lachemi et al. 2004). As the work completed in this thesis is focused primarily on the physicochemical changes in suspensions caused due to changes in cement constitution, the focus of this literature review will be primarily aimed at these influences. A bunch of factors influence the rheological behavior of cementitious system when an admixture is present: the inclusion of mineral admixtures, the inclusion of pozzolanic materials, and the size and shape distribution of the particles present in the suspension. Exploring these factors would aid in understanding the behavior of the systems discussed in this thesis.

The minimum stress required to initiate the flow in the material is called the yield stress or static yield stress of the material. Yield stress immediately after mixing can be attributed to resistance offered by the internal structure comprising of agglomerates of cement grains and weak inter-particle forces (Subramaniam and Wang 2010).

It is noted that several of these rheological studies consisting of cement replacement materials in Portland cement demonstrate conflicting results. Studies conducted by Nehdi (Nehdi and Rahman 2004) showed that at 25% replacement by fly ash resulted in reduction of yield stress at w/p ratio of 0.5, whereas it was observed to increase at w/p ratio of 0.4.

Ferraris (Ferraris, Obla, and Hill 2001) found an enhancement in flowability with use of ultrafine fly ash, reducing the need to use high range water reducing admixture. In both the studies the type of fly ash used wasn't mentioned. The use of Class C, or high calcium fly ash, resulted in a general decrease in flowability of the suspension (Grzeszczyk and Lipowski 1997). In general cement replacement by class F fly ash results in decrease in yield stress and plastic viscosity. Pack found from his investigations that yield stress decreases but there is an increase in plastic viscosity when cement was replaced by class F fly ash (Park, Noh, and Park 2005). The reason for this may be the variability of material, differences in experimentation, differences in chemical admixtures, and possibly issues with the rheological models themselves.

2.7 Microstructure Modeling.

Microstructure modeling was carried out using a 3D particle packing code developed at ASU. The code uses the available particle size distributions of the mixture constituents and carries out a random packing procedure to generate a 3D representative volume element. The overall packing fraction of the constituents is determined from the water to solids ratio to be used in the actual mixtures. The particle size distributions of constituents are discretized to get the number density of each phase in the mixture and the particles are then randomly arranged starting from the largest particle first. The program uses periodic boundary conditions to carry out the packing. For the purpose of the program it is assumed that all particles are spherical in nature. Key microstructural features extracted after packing such as nearest neighbor and contact fractions help understand the progress of hydration reaction at early ages. For any particle, the nearest neighbor is defined as a particle that lies either wholly or partially in the radial field of that particle, defined as a

field with a radius of (r+5) μm, where 'r' is the radius of the particle. The particle contact fraction is calculated as the fraction of nearest neighbor pairs in the microstructure. Cement paste hydration is carried out using the cement hydration package CEMHYD3D (Bentz 2000). The virtual microstructures generated are entered into CEMHYD3D to get the hydrated microstructures at successive time intervals. The hydrated microstructures contain vital information about the location and volume fraction of products formed. The hydration results at particular time intervals are then post-processed to yield the pair contact fractions of certain initial constituents and reaction products. The pair contact fraction is defined as the percentage of one constituent in the radius of influence of another constituent. However, here the radius of influence is varied from 1 micron to 25 microns and a complete plot is obtained for the variation of contact fraction with the radius of influence. This is done because post the initiation of hydration, the particles initially assumed to be spherical cease to remain as spheres due to the formation of hydration products and hydration reactions occurring on the surface and through diffusion. The contact fraction plots thus obtained can be compared at different time intervals to understand the progress of the hydration reaction and the effect of product formation on the rheology of the cement paste.

3 MATERIALS, MIXTURE PROPORTIONS AND TEST METHODS

This chapter contains the description of materials used to form the different blends which were used for research in this thesis. The experimental procedure used is also discussed in detail and the analysis method is explained in brief.

3.1 Materials

This study was performed using a wide variety of materials, including: ordinary Portland cement, limestone, metakaolin, class F fly ash, class C fly ash and Glenium 7500 superplasticizer. As these materials varied for each section of the project, individual materials sections in each chapter have been listed and explained for information on the materials used in this work.

3.2 Experimental Methods

As with materials, experimental methods varied significantly, particularly with respect to rheological characterization of these materials. Based on this, a broad overview of the experimental methods used in this dissertation is provided. For a more in depth look that the experimental methods used in each section, the author directs the reader to the experimental methods sections in each chapter.

A wide variety of rheological experiments was conducted as part of this study, for detailed information on the individual experiments the readers can be directed to the respective chapters where those experiments were completed. Thus, to avoid confusion relating which experiment was conducted as a part of which test, the discussions here will focus on the instrument and geometries used in these experiments. The rheometer used in this study is a TA Instruments AR2000EX dynamic shear rheometer, the instrument is pictured in Figure 8.

Figure 8: TA Instruments AR2000EX used in this Study, shown in Vane Geometry Configuration.

The rheometer consists of a base which has a cup apparatus at the bottom and the configuration used was Peltier steel vane geometry. The cup is temperature controlled and for our experiments it was set to 25ºC using a chiller apparatus. The other part of the rheometer is the geometry, the geometry used in this thesis was Peltier steel vane geometry with 4 vanes. The vane geometry consists of a 28.04 mm diameter and 42.01 mm length. The cup has a diameter of 30mm in which the material of volume 45 mL is loaded. Vane geometry is used to avoid slip between the sample and the sides of the cup. The cup-and – bob geometries used in this study are pictured in Figure 9.

Figure 9: Cup-and-bob Geometries used in Study

4 TIME DEPENDENT RHEOLOGICAL RESPONSE OF OPC-SCM BINDERS WITH ADDITION OF SUPERPLASTICIZERS

4.1 Introduction.

As mentioned earlier SCMs have found to be a viable partial replacement to OPC and are thus used on a large scale in construction industry. They have advantages on the durability and strength of cement concrete. This chapter evaluates the rheological early age properties of these OPC-SCM blends over a period of two hours. The chapter also discusses the influence of superplasticizer on these blends along with addition of limestone. The parameters that have been evaluated are yield stress, plastic viscosity and storage modulus.

4.2 Experimental Program.

4.2.1 Materials and Mixture Proportions.

The materials used include Type I/II ordinary Portland cement (OPC) conforming to ASTM C 150, Class F fly ash conforming to ASTM C 618, Class C fly ash and a nominally pure limestone powder conforming to ASTM C 568.

Here Class F fly ash is purely pozzolanic material whereas class C fly ash has both pozzolanic as well as hydraulic properties. Limestone is used as a filler to reduce costs and make the paste more sustainable. For ternary blends a superplasticizer was utilized to improve the flow and then compare it with binary blends and conventional OPC. Figure 10 shows the particle size distribution of OPC, Class F fly ash, Class C fly ash and limestone, as measured using laser diffraction, along with their median particle size. Blaine's surface area for each material was found using Blaine's fineness test.

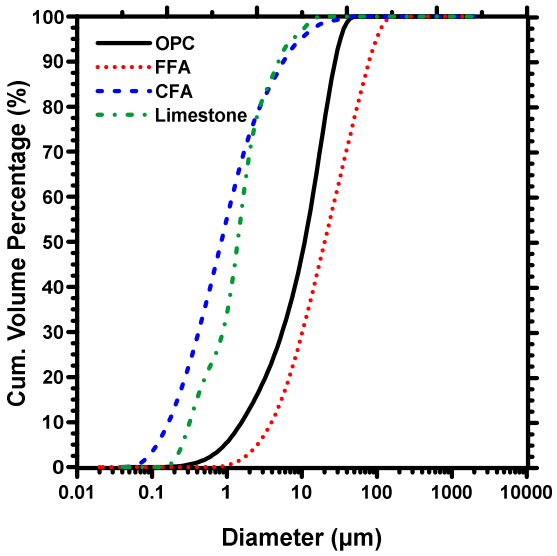

Figure 10: The Particle Size Distributions (PSD's) of OPC, Class F fly ash, Class C fly ash and 0.7 micron Limestone.

OPC (D_{50} = 10.9 µm) FFA (D_{50} = 19.9 µm)

CFA (D_{50} = 0.79 µm) LS (D_{50} = 1.4 µm)

The composition of ordinary Portland cement and other replacement materials are given in Table 5. The CaO content in the fly ash is way less than OPC, whereas the silica and alumina content is much higher in fly ash particularly class F fly ash. Fly ash have well defined spherical shape and has a glassy surface. OPC particles are highly angular and contain phases such as C_3S, C_2S, C_3A and C_4AF. C_3A and C_3S are a very important constituent as far as early age rheology is under consideration. The specific gravity of OPC, class F fly ash, class C fly ash and limestone are 3.15g/cc, 2.34 g/cc, 2.54 g/cc and 2.7 g/cc respectively.

For all the cementitious suspensions considered, cement was replaced by either limestone or fly ash on a volumetric basis to ensure that the comparisons are consistent. The suspensions were prepared at a constant mass-based water-to-solid ratio $(w/s)_m$, of 0.4. A

polycarboxylate chemical admixtures was used in ternary blends to study its effects on the rheology.

Table 5: Composition and Specific Surface Area of Raw Materials used in the Study.

Phase (%)	OPC	Class F fly ash	Class C fly ash	Metakaolin
SiO_2	21.06	59.31	35.5	51.52
Al_2O_3	3.86	22.94	19.62	40.18
Fe_2O_3	3.55	4.63	5.96	1.23
CaO	63.75	5.31	23.04	2.0
MgO	1.83	-	4.04	0.12
SO_3	2.93	0.47	2.78	0.0
Na_2O	0.12	1.43	-	0.08
K_2O	0.48	-	-	0.53
LOI	1.99	0.68	0.79	2.01

Limestone powder contains 95-97% $CaCO_3$ with a Blaine's surface area of 4970 m^2/kg. Binary blends comprised of mixes with replacement of OPC by Class F fly ash and Class C fly ash in the range from 20 to 50%. In case of ternary blends OPC was replaced by Class F fly ash in the range of 20 to 40% and 10% of limestone by volume. Also in the ternary blend, a superplasticizer was added at 0.8% of volume of solids. The mix composition of different blends is tabulated in Table 6. All binary pastes were maintained at fixed water to solids ratio $(w/s)_m = 0.4$ and the ternary pastes were mixed at a $(w/s)_m = 0.3$ to maintain

the same fluidity as of the binary blends. This was ensured using a simple flow test. Therefore a comparative study of rheological properties of various pastes when the flow is the same as confirmed by preliminary tests, is possible.

Table 6: The Proportions of the Paste Mixtures Evaluated in this Study.

Mix type	Replacement level (% by volume)		
	Class F fly ash	Class C fly ash	Limestone
OPC	-	-	-
OPC+FFA	20, 35, 50	0	0
OPC+CFA	0	20, 35, 50	0
OPC+FFA+LS	20, 30, 40	0	10

4.2.2 Rheological Procedure.

All powders are dry mixed thoroughly before adding water. Mixing procedure followed was as per ASTM C 1738. Following procedure was used to mix (1) After adding water materials were mixed at low shear rate for 30 s (2) the mixer was run at high shear for 30 s (3) The mixer was opened and the dry material was scraped off the walls of the mixer and allowed to rest for 2 min with the lid closed (4) The mixer was then run at high shear for 90 s. At the end the homogeneity of the paste was verified by hand mixing it again. Around 45 mL of sample was injected into the rheometer using a syringe and covered with a cap to disable loss of water due to evaporation. The time elapsed from water addition to the beginning of the rheological assessment was approximately 5 min.

The instrument used to conduct the experiment is a stress controlled rheometer (AR 2000

EX). The rheometer consists of a base which has a cup apparatus at the bottom and the configuration used was Peltier steel vane geometry. This reduces the slippage at the walls of the geometry. The temperature of the cup was maintained at 25 ± 0.5 °C. Strain controlled mechanism was used to evaluate the yield stress and plastic viscosity of the material. After injecting the material into the cup the rheological procedure consisted of ramp-up pre shear strain rate from 0.005/s to 100/s to homogenize the material., followed by a ramp up at the desired time after injecting the material from 0.005-to-100/s, and followed immediately by a ramp down from 100-to-0.005/s. Such wide range of shear-rate substantially improves the prediction of yield stress (Vance, Sant, and Neithalath 2015). A step up, or step down shear rate of 10/s was implemented, as shown in Figure 11. Shear stress and shear rate data were extracted using TA Instruments' TRIOS software package. With the exception of the pre-shear range, at each step, data is acquired every second, until a steady state is achieved — as defined by three consecutive torque measurements within 5% of each other, at which time the experiment advances to the next shear rate. The time at each shear step is typically 5 s. For time dependent study the material was injected into the cup and pre shear was performed to discard the air bubbles and the vane was allowed to stay in the material for the duration before the ramp up begins. The procedure to determine the yield stress was adopted from (Vance et al. 2013). The plateau region achieved at low strain rates of the ramp up side is considered to be the yield stress. Plastic viscosity is the slope of the line formed by ramp down values between the shear rate range of 5/s and 100/s. This method of obtaining yield stress and plastic viscosity were reliable compared to the conventional models as the material behaves non-linearly.

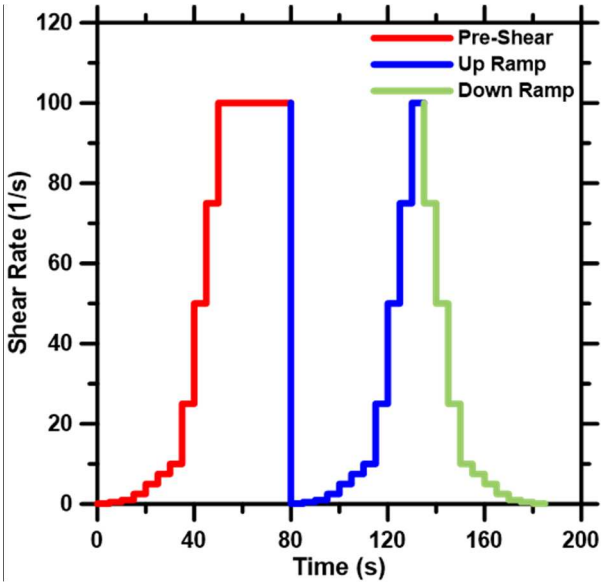

Figure 11: The Rheological Procedure for Shear Rate Ramp Study (K. Vance 2015).

In case of oscillatory method, stress controlled mechanism was used to find storage modulus and loss modulus. An oscillatory stress was applied from 0.005 Pa to 100 Pa at a constant frequency of 1 Hz. The flat region of constant shear modulus before the drop is the true value of storage and loss modulus. The values of G' and G'' were extracted from TRIOS software.

4.3 Results and Discussion.

4.3.1 Comparative Analysis of Class C & Class F fly ash on Yield Stress.

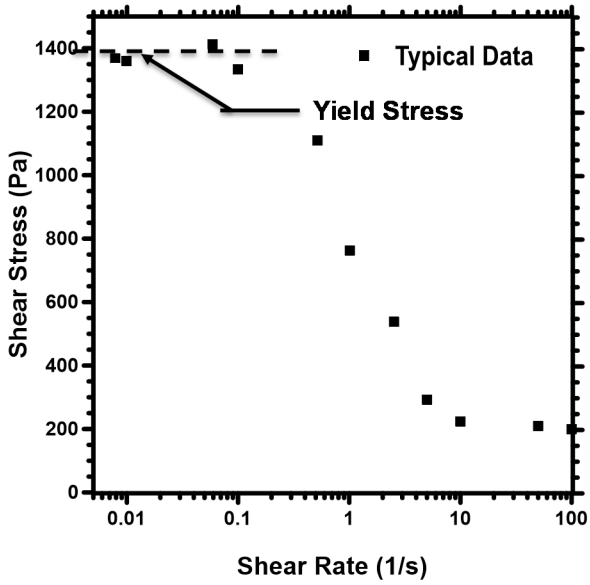

Figure 12: Stress Plateau Method to Measure Yield Stress.

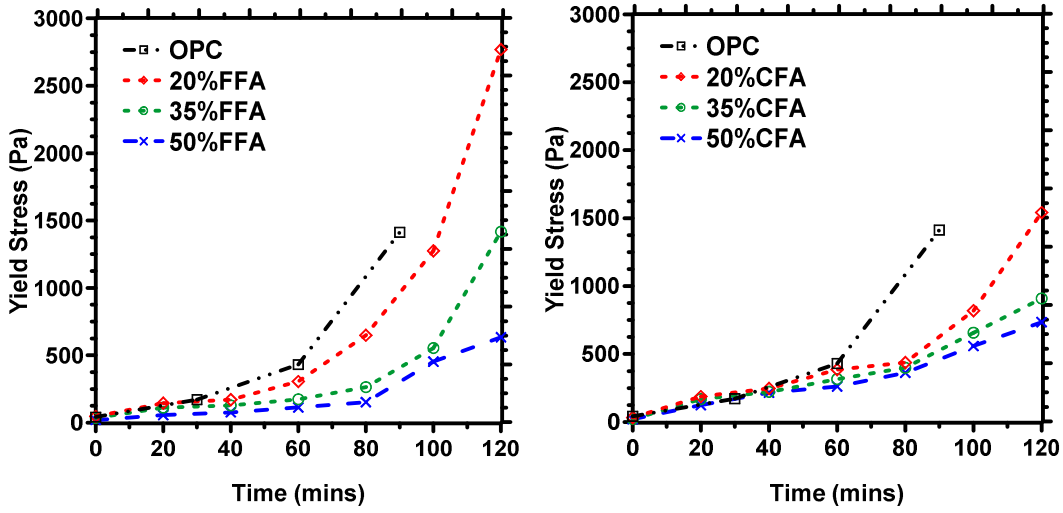

Figure 13: Time Dependent Influence on Yield Stress a) OPC-FFA and b) OPC-CFA Blends.

It was seen that these values of yield stress are decreasing with increase in replacement of class F fly ash. Cement particles have a strong tendency to flocculate, a finite stress needs

to be applied to de-flocculate it and induce flow and is defined as the yield stress.

From Figure 13, we can observe that yield stress at different replacement levels of FFA increase with time which is similar to results obtained by Subramaniam (Subramaniam and Wang 2010). However, this increase is more prominent at low replacement. For 20% replacement, it can be seen that up to 60 mins the increase is gradual which later gets steep with time. A similar trend can be seen for other replacement levels, for 35% and 50 % replacement with FFA the steep increase is seen after 80 mins. Comparing these values with conventional OPC, OPC yield stress increases drastically from 60 mins. At all times it is clearly seen that yield stress values go down with increase in replacement level. The same trend is seen after 40 mins with that of replacement with class C fly ash, until 40 mins there is no particular difference in the yield stress between different blends of CFA and OPC. The surge in yield stress values in CFA blends is seen after 80 mins but the rate of increase is inversely proportional to the OPC replaced by CFA in the blends. Results of OPC could be obtained only up to 90 mins due to the limitation of the instrument. Comparing the results of FFA replacement with that of CFA replacement it is evident that FFA blends have lower yield stress up to 80 mins in case of 35% and 50 % replacement after which 35% FFA blend has much larger yield stress than 35% CFA blend but the at 50% replacement both blends show similar yield stress. For 20 % replacement blends, FFA displayed lower yield stress until 60 mins after which it augments at an enormous rate compared to 20% CFA blend. At all times, the yield stress of the blends are always less than that of OPC.

The composition of OPC, class F fly ash and class C fly ash are given in Table 5.The CaO content in the fly ash is way less than OPC whereas the silica and alumina content is much

higher in fly ash particularly class F fly ash. Fly ash have well defined spherical shape and has a glassy surface. OPC particles are highly angular and contain phases such as C_3S, C_2S, C_3A and C_4AF. C_3A and C_3S are a very important constituent as far as early age rheology is under consideration.

Immediately after mixing, the paste is a viscous fluid with comparatively less resistance to shear, the particles are comparatively far apart, which means low packing density and the yield stress is solely dependent on weak inter-particle forces which results in low yield stress. It is seen from previous work that the attractive force between OPC particles is much greater than that of fly ash particles or between OPC-fly ash particles. Infact the force is the least between OPC- fly ash particles. This early gradual development of yield stress can be attributed to the formation of ettringite by reaction of C_3A with gypsum. Ettringite are needle like particle and thus have very good interlocking and provides rigidity to the paste. With higher replacement by FFA the C_3A content reduces as C_3A is a component of OPC and thus less ettringite formation takes place leading to lower yield stress. Finally, the potential for agglomeration also reduces with increasing particle size (replacement by FFA), reducing the possibility of water remaining trapped within flocs, where it is unavailable to provide fluidity to the cement paste. The number of flocculated cement particles to the cement particle connection reduces, this causes a dilution effect. Yield stress values are dominated by properties of cement particles.

The point at which the yield stress drastically increases is called the rheological setting point. This sudden surge in the yield stress is because of solid structure formation, hydration of cement has begun and C-S-H formation is initiating. There is continuous increase in formation of hydration product around the cement particles which utilizes the

water in the system and in turn reduces the free water. The particles now grow as C-S-H is formed over the cement particles which in turn reduces the distance between the particles increasing solid-solid attractive forces and consequently the yield stress. In OPC-FFA blends there is formation of C-S-H at the same time as OPC as conformed from isothermal calorimetry tests. The onset of acceleration phase of OPC and the blends is seen to occur at the same time with decrease in heat evolution with increase in replacement. The reduced heat formation indicate reduced C-S-H formation which in turn reduced the yield stress of the blends at later ages.

The mineral components of high calcium fly ashes, unlike those detected in low calcium ones, are the same crystalline phases one may find in cement, i.e. C_3A, C_2S, C_4A_3S, $C_{12}A_7$, C_2F, $CaSO_4$, free CaO (Grzeszczyk and Lipowski 1997).

Thus at early ages just as cement particles have better inter-particle forces of attraction even class C fly ash has a better inter particle attraction force as compared to class F fly ash due to presence of phases like cement. This attractive forces between class C fly ash cause it to agglomerate when mixed with water. Slowly there is reaction of C_3A with gypsum to produce ettringite which have needle like structure. This imparts the early age yield stress to the blends. As mentioned earlier there is no C_3S phase in class C fly ash which in cement undergoes hydration to form thin film of C-S-H which causes the tremendous increase in yield stress. In class C fly ash blends in 35 and 50% replacement blends the surge in the yield stress absent until 120 minutes. This is due to delay in the onset of acceleration phase in blends compared to OPC. The onset for 35 ad 50% class C fly ash blends was seen to occur at 140 mins and 180 mins respectively. As there is increasing formation of products like ettringite and C-S-H in the paste the packing density

increases and the inter particle distance reduces which increases the resistance of the suspension to applied shear. Moreover, in binary pastes containing particles finer than OPC as in the case of class C fly ash, agglomeration and water film formation are expected to be substantial, and would decrease the amount of free water available in the paste (Sakai et al. 2009).

4.3.2 Comparative Analysis of Class C & Class F fly ash Blends on Plastic Viscosity.

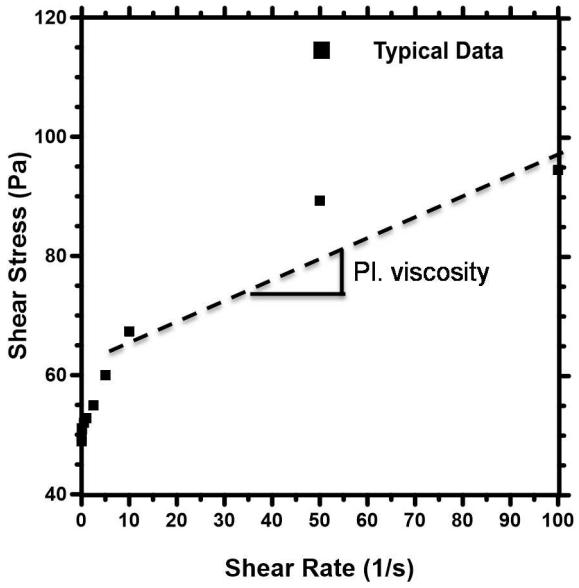

Figure 14: Procedure to Obtain Plastic Viscosity.

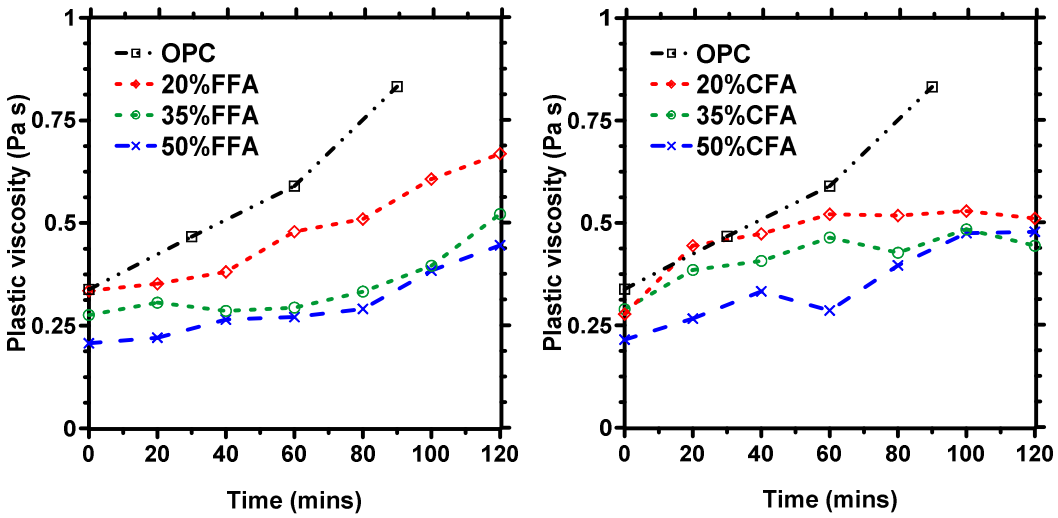

Figure 15: Time Dependent Influence of Replacement of OPC-FFA and OPC-CFA on Plastic Viscosity.

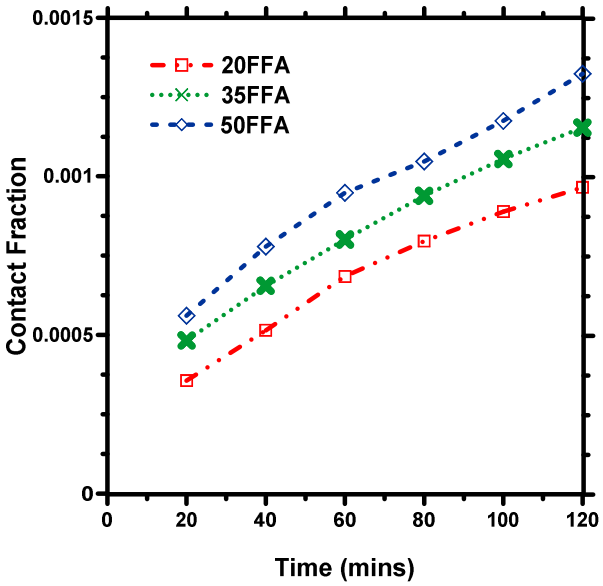

Figure 16: Contact Fraction between FFA-Ettringite Particles with Respect to Yime.

The procedure for evaluating the plastic viscosity of the mix is shown in figure 14. The slope of the strain rate v/s stress curve for points of strain rate between 5/s to 100/s is considered to be the plastic viscosity (Vance et al. 2013). From Figure 15, it can be noted

that the plastic viscosity for OPC paste increase at a higher rate with time as compared to plastic viscosity of samples with replacements. 20% replacement also has comparatively high rate of increase of plastic viscosity with time where as 35% and 50% has low rate of increase plastic viscosity.

In class C fly ash, 20% and 35 % blends show similar increase in plastic viscosity as of OPC at very early age up to 30 mins after which there is gradual increase until 120 mins which is opposite to class F blends. 50 % CFA blend shows constant increase in plastic viscosity and at the end of 120 mins has similar values as that of 20% and 35 % blends.

FFA-Ettringite contact fraction increases with replacement and time as seen in Figure 16.

Plastic viscosity of a non-Newtonian is mainly a factor of the particle shape of the suspensions in the liquid. In our pastes cement is the major constituent which is angular in shape which in turn provides good interlocking among the particles causing more resistance to flow. The second suspension particle in our mix are the fly ash particles which are spherical in shape and thus have a ball bearing effect which imparts fluidity to the paste. The degree of contact between cement particles influences the PV more than the contact between other particles. This effect is reduced by increasing content of fly ash in the paste because of its spherical nature which compensates against the viscosity enhancing effects (Vance et al. 2013).

Class F fly ash as seen from the PSD's are coarser than cement and thus the separation between particles is much larger, similar to the behavior of the paste with coarse limestone, which reduces the yield stress and plastic viscosity (Vance et al. 2013).

Class C fly ash particles are comparatively finer than OPC and thus increases overall packing density reducing particle spacing. This in turn increases the inter-particle contact

and elevates plastic viscosity.

The initial slow growth of PV in case of class F blends which is the dormant phase is only due to the formation of ettringite which are needle like particles and have strong interlocking effect which in turn contributes to high friction compared to spherical particles of fly ash. In these blends as the C_3A required to form ettringite is less compared to class C blends because it has C_3A in both fly ash as well as in OPC. Thus we can see that at very early age just after mixing class C blends have higher rate of increase in PV. Class F fly ash particles are also coarser than OPC thus have less contact fraction which causes the plastic viscosity to augment at a slower rate. In class F and 50% replacement by CFA blend there is a slow growth rate which can be attributed to the spherical nature of fly ash particles which compensate the effect of ettringite formation.

As we move forward in time, formation of C-S-H around the cement particles increases the surface area. As the surface area increases (or the effective particle size decreases), and inter-particle spacing decreases, there is an increase in the number of inter-particle contacts and inter-particle friction, and thus plastic viscosity.

At later ages as mentioned in previous section C-S-H formation in case of class F fly ash is much faster than class C fly ash as it is more pozzolanic due to presence of high content of silica and alumina. This is the reason for faster rate of increase of PV at later ages as compared to class C fly ash. C-S-H has a very large surface area and thus causes high friction among particles trying to flow and thus high PV. The spherical class C fly ash along with low C-S-H formation can be said to be the reason for slow growth of PV.

4.3.3 Comparative Analysis of Class C & Class F fly ash on Storage Modulus.

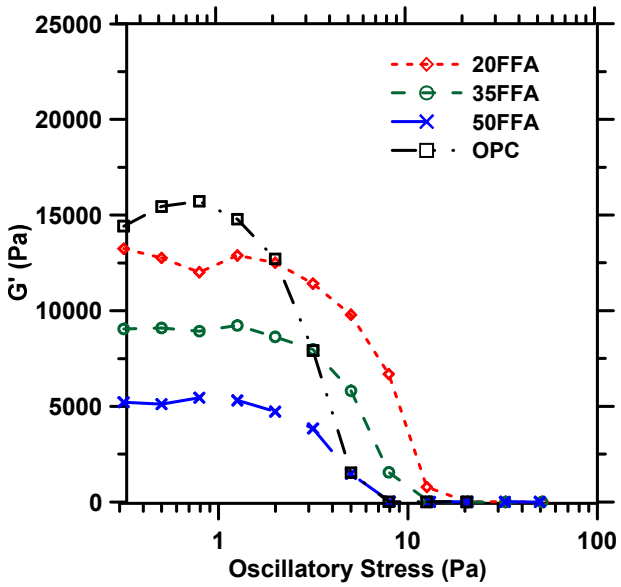

Figure 17: Representative Storage Modulus Curves for OPC and OPC-FFA Blends with 20, 35 and 50% Replacement.

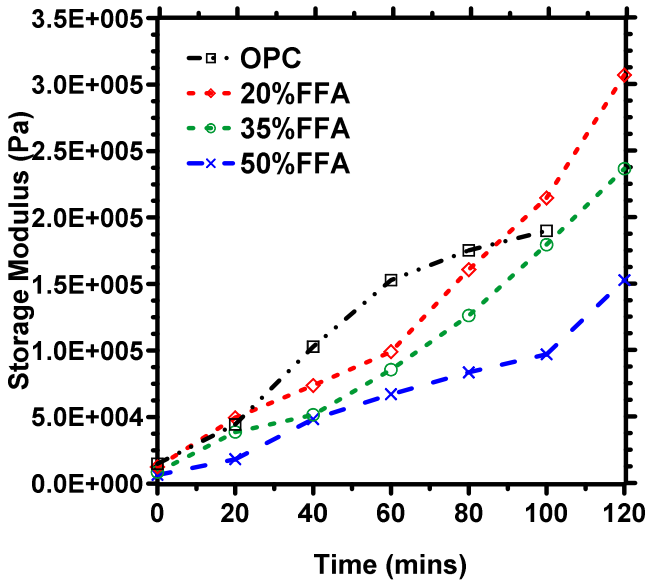

Figure 18: Time Dependent Influence of Replacement of OPC by Class F Fly ash on Storage Modulus.

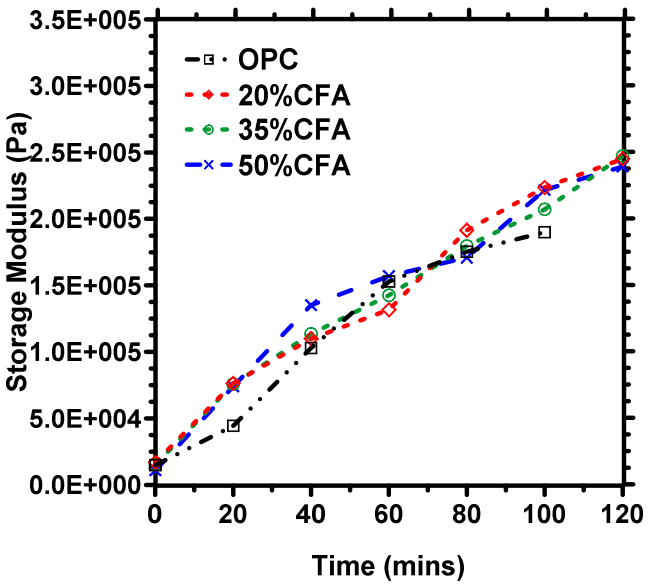

Figure 19: Time Dependent Influence of Replacement of OPC by Class C Fly ash on Storage Modulus.

Storage modulus is an important characteristic of cement paste which represents elastic properties of the material. During experimentation it is taken care that the stress applied is within the linear visco-elastic region (LVER) because once the stress is applied above this minimum stress, the material begins to flow plastically (Subramaniam and Wang 2010). Under plastic conditions these parameters that are found using rheometer are not precise and cannot be depended on. Under low oscillatory shear stress of the vane we find an almost constant G' which then decreases as it moves from the elastic to plastic regime as the applied stress is increased which causes a gradual breakdown of the structure. From Figure 17 we can see that for different proportions of Class F blends the values of G' falls with increasing replacement, also the length of the constant G' also is shorter as the replacement increases which means the elastic region is diminishing.

From Figure 18, 19 it can be seen that G' increases with time in all the blends. In case of

class F blends its observed that with increase in replacement of OPC with class F fly ash, the rate of growth of G' with time is comparatively slower. This characteristic can be attributed to the volume of solid particles in the blended pastes which will be explained later in detail. After 90 mins it is observed that the G' of 20% class F blend is higher than OPC which will also be answered in the following paragraphs. Class C fly ash blends on the other hand grow at the same rate and have similar G' at different time period. The values are same as that of OPC throughout the time span, again after 90 mins trend similar to class F fly ash is seen in which the blends have higher G' than OPC.

The ionic strength of the system increases due to continuous dissolution of anhydrous cementitious phases, this causes the cement particles to re-agglomerate and increases G' over time. In case of class F blends the initial slow growth of G' is due to flocculation of cement particles. This period is known as the induction period, after which there is a slightly faster rate of increase of G' due to formation of higher volume of hydrates, especially the high specific surface area C-S-H. Earlier studies report that a hydration layer is formed on the surface of cement grains including a layer of Al-Si rich gel, C-S-H and AFt phases (Betioli et al. 2009). C-S-H gel causes intense agglomeration due to increase of van der Walls force and the structure is formed by coagulated particles, this is the beginning of the acceleration phase as confirmed by calorimetry tests.

Class F fly ash are coarser than OPC therefore occupy larger volume in the paste, thus during volumetric replacement less number of fly ash particles replace the same volume of OPC thus the number of particles in the paste reduces leading to lower packing density and lower volume of solids which causes reduction in elastic properties of the paste. The G' increment with time is due to formation of ettringite at very early age followed by C-S-H

structure formation. In case of class C fly ash which are finer than OPC have a better packing density so the G' values are higher at early ages where ettringite formation is similar. The G' values are similar to OPC at later ages because C-S-H formation in class C blends are less compared to OPC but higher packing density and volume of solids in the class C blends compensates for lower C-S-H.

4.4 Effects of Superplasticizers (SP) on the Rheological Response of SCM-OPC Blends.

In case of high performance concrete (HPC), various superplasticizers are used to enhance the workability of the mix. Only by using superplasticizers can rheological properties of HPC mix be modified for concrete processing. Thus, the key element in efficient workability shaping is the complex knowledge of how superplasticizers influences the rheological properties of fresh concrete in different casting conditions.

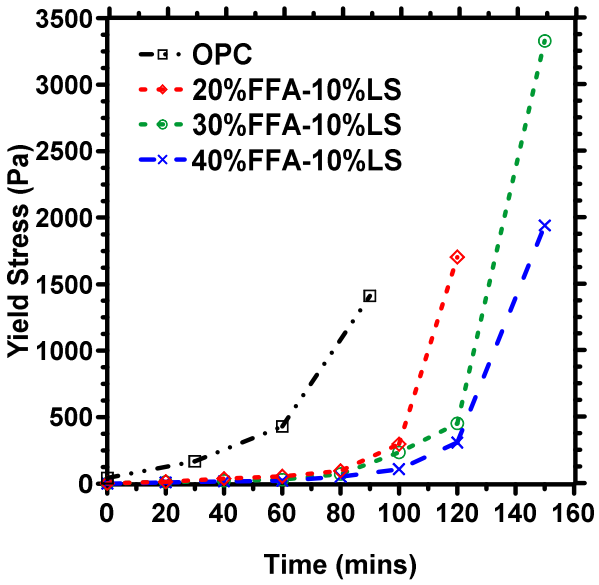

Figure 20: Yield Stress of Ternary Blends with SP with Respect to Time.

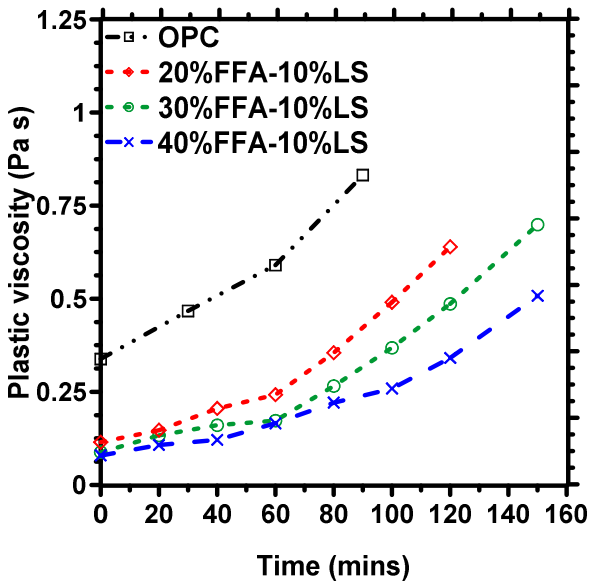

Figure 21: Plastic Viscosity of Ternary Blends with Time.

The effect of superplasticizers can be very well explained using yield stress and plastic viscosity values as seen in Figure 20 and 21. It is observed that the yield stress values have significantly reduced with addition of superplasticizer compared to OPC. In Figure 20, a graph of blends with superplasticizer shows the increase in yield stress with time. The yield stress values for 20% fly ash blends increase gradually until 100 mins after which there is a high rise in the yield stress. In case of 30% and 40% blends this rise is seen at 120 mins. The effect of the superplasticizer reduces beyond this point and thus the jump in the yield stress is attributed to the end of the effect of superplasticizer. The yield stress values decrease with an increase in replacement of OPC by fly ash which is similar to the results of previous section.

Figure 21, represents the trends in plastic viscosity of OPC-SCM blends with superplasticizer. There is a decrease in the plastic viscosity with increase in replacement by fly ash but the rate of increase is similar to OPC mix. Similar trend was observed with

binary blends without superplasticizer, but the plastic viscosity values in ternary blends with superplasticizer are lower than the binary blends without superplasticizer.

The localized surface charges on OPC promote flocculation of hydrating cement particles, but they can be effectively neutralized and separated by the anionic charge of the SP molecules. The hydration of interstitial phases is affected by the concentration of Ca^{2+}, OH^- and SO_4^{2-} ions in suspension in water (Chandra and Björnström 2002). The concentration of those ions depends upon the amounts of alkali sulfate, gypsum and free lime in the cement just after mixing with water, followed by the hydration reaction of C_3S, alite. The relative sizes of the particles in a cementitious system with a suspension of SP molecules differ typically by two or three orders of magnitude; the average diameter of cement particles are typically of 10 micron, whereas the size of the SP molecules is of the order of a few nanometers.

The admixture is unevenly adsorbed on cement containing more of $C_3A + C_4AF$ that the amount of admixture adsorbed on alite and belite is relatively decreased, thereby lowering the fluidity of the paste. The more even the adsorption of admixture on cement minerals, the higher the fluidity of the paste will be. Thus, the amount of the admixture adsorbed on the cement sometimes fluctuates greatly, as it depends on the mineral composition of the clinker (S. Chandra 2002).

Thus it can be explained that until 100 mins when there is ample amount of C_3A in the mix the SP are adsorbed on it and reduces the yield stress after which the reduction in C_3A content due to conversion to ettringite there is a high growth in yield stress. The plastic viscosity of the paste with SP is lower than blends without superplasticizer because they separate the particles inducing large inter-particle spacing which in turn imparts fluidity to

the mix.

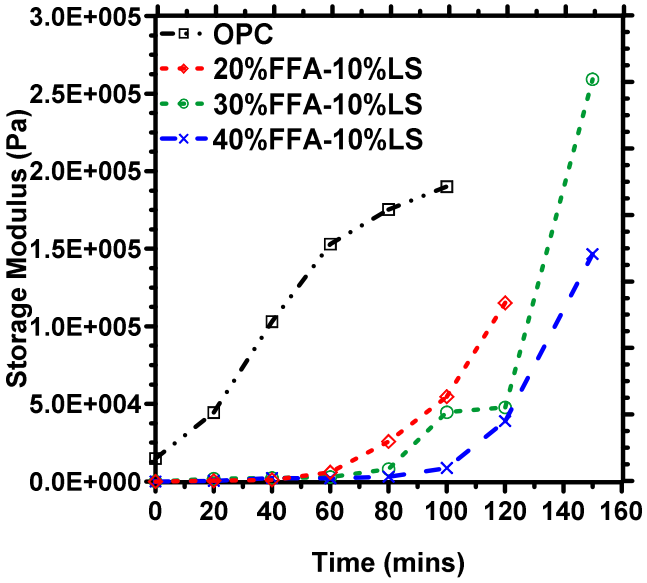

Figure 22: Storage Modulus of Ternary Blends with SP with Respect to Time.

Superplasticizers have a huge influence on the storage modulus of the ternary blends. The relationship between time and storage modulus is shown in Figure 22. With the data obtained, the figure seems to show a significant difference between values of storage modulus of pure OPC compared to ternary blends with superplasticizers. The storage modulus of ternary blends is way less than that of OPC until 100 mins. In 20% fly ash blends the G' value begins to elevate after 60 mins whereas in 30% and 40% fly ash blends G' rises after 80 mins. At all times the storage modulus values with higher replacement are always less than lower replacement.

SP molecules are made of long chains and links which attaches to cement particle which is known as the adsorption phase. The long chains separate the particles and fluidizes the mixture which is also known as steric repulsion. Consequently, electrostatic repulsion occurs between the cement particles. The cement particle arrangement in a paste matrix

offsets the inter-particulate attractive forces (Heikal et al, 2005). As reaction takes place in which ettringite is formed on the surface of the cement particles which equilibrates the effect of SP.

Polycarboxylate superplasticizer (PCS) is an anionic surfactant, when adsorbed on cement particles become negatively charged causing a repulsive effect among the particles, consequently its fluidity increases; in addition, the side chains preserve water molecules in contact via hydrogen bonding creating osmotic pressure which increases the movement of these cement particles. PCS improves the fluidity of cement pastes by the dispersion of cement particles. The adsorption of PCS superplasticizer molecules on the cement particles hinders their flocculation as a result of the electrostatic repulsion forces and/or through steric hindrance. Consequently, the particles are homogenously distributed in the aqueous solution, minimizing the amount of water needed for them to be dispersed, which leads to the higher fluidity and workability of cement pastes (Uchikawa et al, 1997, Jolicoeur C 1994).

According to Mollah et al., the delay in growth of G' could be due to the dispersive action of the PC admixtures among the cement grains changes growth kinetics and morphology of hydrate phases.

5 RHEOLOGICAL RESPONSE OF IRON BINDER SYSTEM

5.1 Materials and Mix Proportions

The materials used for this study are Iron powder (fine and coarse) which is a bag house dust waste during the manufacturing process of steel. Metallic iron powder with median particle size of 19 μm is used as the main starting material in this study. The iron powder is obtained from a shot-blasting facility in Phoenix, AZ. The iron powder has mostly elongated and plate-like particles as can be seen from the scanning electron micrograph as shown in Figure 23, thereby influencing the rheological properties of the mixture. However, the larger surface area-to-volume ratio of this shape as compared to the spherical shape provides benefits related to reactivity. The iron powder consists of 88% Fe and 10% O (some amount of atmospheric oxidation) along with trace quantities of Cu, Mn, and Ca.

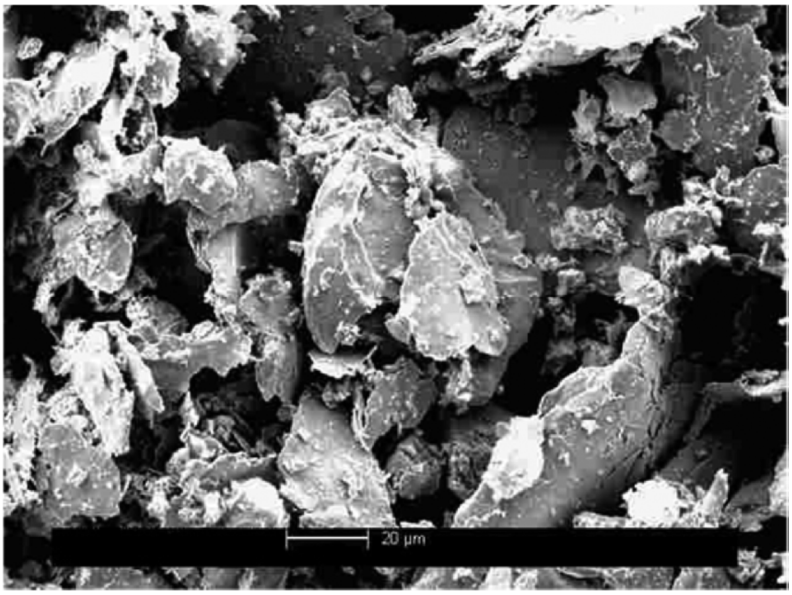

Figure 23. Scanning Electron Micrograph of Iron Particles. The Scale Bar Corresponds to 20 μm.

The other materials used in the binder include class F fly ash and metakaolin conforming to ASTM C 618, and limestone powder with a median particle size of 0.7 μm conforming

to ASTM C 568. To minimize the water demand, yet keeping the consistency and cohesiveness of the mixture, metakaolin was used. An organic reducing agent- oxalic acid, for metal cations was also used. The particle size distributions of the iron powder, fly ash, metakaolin, limestone powder and OPC, obtained from a laser diffraction-based particle size analyzer are shown in Figure 24. All the ingredients are finer than the iron powder used. The composition of metakaolin is represented in tabular form in Table 1.

Metakaolin has very fine particle size compared to other particles in the mix and it has very good pozzolanic characteristics. Fly ash has been chosen to make use of its spherical shape that enhances the workability characteristics of the suspension.

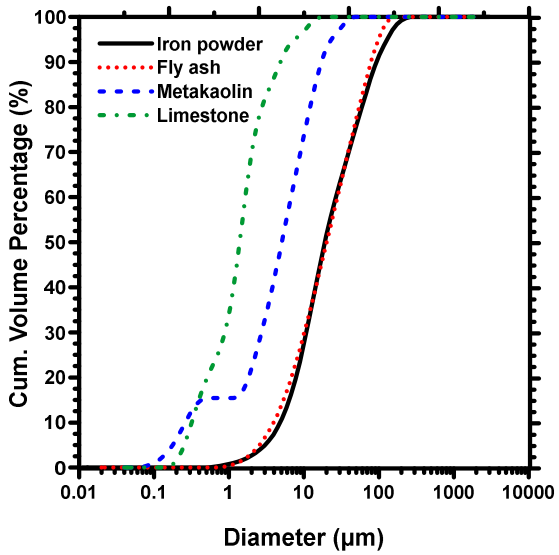

Figure 23: Particle Size Distribution of Fly ash, Metakaolin, Limestone and Iron Powder.

The study containing class F fly ash, metakaolin, limestone, Iron powder involved various mixes to explore the effects of fly ash and metakaolin on the rheology of the binder system. Preliminary mixes were tested to identify that fly ash and metakaolin have a major influence on the yield stress and plastic viscosity. Thus, to study these effects in detail, 16 mixes were prepared with composition of fly ash varying from 0 to 20% and metakaolin

from 0 to 10%. Limestone was kept constant at 10% and the rest of the mixture containing iron powder which ranged from 60 to 90%. The reducing agent, oxalic acid was added to all mixes at 2% by mass. The specific gravity of iron powder, metakaolin, fly ash and limestone are 3.54g/cc, 2.5g/cc, 2.34g/cc and 2.7g/cc respectively. All the replacements for this study were mass based and a water to powder ratio $(w/p)_m$ of 0.35. The mix design for this study is clearly tabulated in Table 7. The effect of iron was studied by keeping the metakaolin and fly ash content constant at 6% and 10% respectively. Iron was varied between 60 to 80% while the rest of the mix comprised of limestone as shown in Table 8.

Table 7: Mix Design for Iron Powder Binder System (MK-Metakaolin, FA – Class F fly ash, LS – Limestone and Fe – Iron).

Mix	**1**	**2**	**3**	**4**	**5**	**6**	**7**	**8**	**9**	**10**	**11**	**12**	**13**	**14**	**15**	**16**
MK	0	0	0	0	3	3	3	3	6	6	6	6	10	10	10	10
FA	0	8	15	20	0	8	15	20	0	8	15	20	0	8	15	20
LS	10	10	10	10	10	10	10	10	10	10	10	10	10	10	10	10
Fe	90	82	75	70	87	79	72	67	84	76	80	72	69	64	65	60

Table 8: Mix Design to Evaluate Effect of Iron in Iron Binder System.

Mix	FA	MK	Iron	LS
FA + MK + Iron + LS	10%	6%	60-80%	4-24%

We will also be looking at the OPC-iron powder binder system in which OPC is replaced by iron powder from 0 to 40% replacement by volume. A water to cement ratio $(w/c)_m$ of 0.5 was used consistently in all the mixes. The mix design is shown in Table 9.

Table 9: Mix Design for OPC-Iron Binder System.

Ordinary Portland Cement Volume %	Iron Powder Volume %
100	0
90	10
80	20
70	30
60	40

5.2 Rheological Experiment

The mixing procedure involves initial dry mixing of all materials (iron powder, fly ash, limestone powder, metakaolin, and the organic reducing agent). Water was then added and mixed to obtain a uniform cohesive mixture. The mass-based water-to-solids ratio (w/s) was kept constant at 0.35 in the mixtures to attain a cohesive mix. The mixture was hand blended for 1 minute before pouring it into the rheometer apparatus. The same rheological procedure for linear shear as well as oscillatory shear experiments as mentioned in previous section is followed.

In case of OPC-iron binder system OPC and iron powder are dry mixed and then added with water. The mixture was hand blended for 1 minute and then injected into the rheometer to begin with the experiment as mentioned above. The rheological experiment carried out was same as mentioned in chapter 4, the only difference being that this was not a time dependent study and thus the linear shear or oscillator shear stress was applied as soon as the paste was mixed and poured into the bob of the rheometer.

5.3 Iron Binder System

5.3.1 Effect of Metakaolin and Fly ash on Rheological Properties.

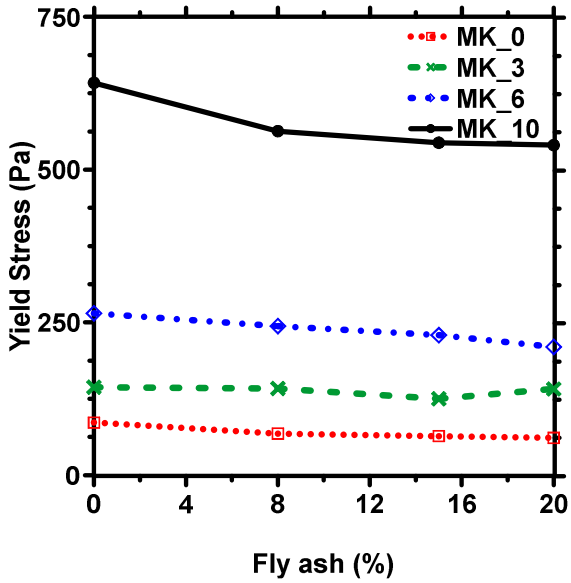

Figure 24: Influence of MK-FA on Yield Stress of Iron Binder.

It is clearly observed from Figure 24 that with increasing metakaolin content from 0 to 10% there is higher increase in yield stress. There is almost an increase of 6 times in the values of yield stress at 10% metakaolin as compared to that of 0% metakaolin. At 0% metakaolin and fly ash, the yield stress observed is purely due to iron particles and limestone powder. As the fly ash content was increased from 0 to 20% there was a subsequent decrease in the values of yield stress which was as expected. The comparative decrease in low metakaolin mixes was greater than in high metakaolin blends. As the metakaolin and fly ash in the mixes is increased at the expense of iron content by mass.

The very high growth of yield stress with replacement by metakaolin can be attributed to the agglomerating nature of metakaolin. A material with a zeta potential between $\pm$30 mV has a tendency to agglomerate when mixed in water. Metakaolin has zeta potential around -15 mV thus have a very strong tendency to undergo agglomeration (Lopez, Sugita et al).

This agglomeration holds the water between these particles and does not leave enough water for other particles to flow through thus increasing the yield stress. With an increase in the fly ash particles into the system, there are more number of spherical particles which have a ball bearing effect and causes reduction in the yield stress. Fly ash particles have less attractive forces between them as stated by many authors. These fly ash particles have a mean diameter of 19 µm compared to a metakaolin particle of 5.1 µm. Thus introduction of such large particles cause the metakaolin particles to move apart leading to a lower agglomeration and lower yield stress. At higher metakaolin levels this effect is less evident because there is a lot metakaolin for which 20% increase in fly ash is not enough to lower the yield stress to an extent which was achieved by blends containing lower metakaolin.

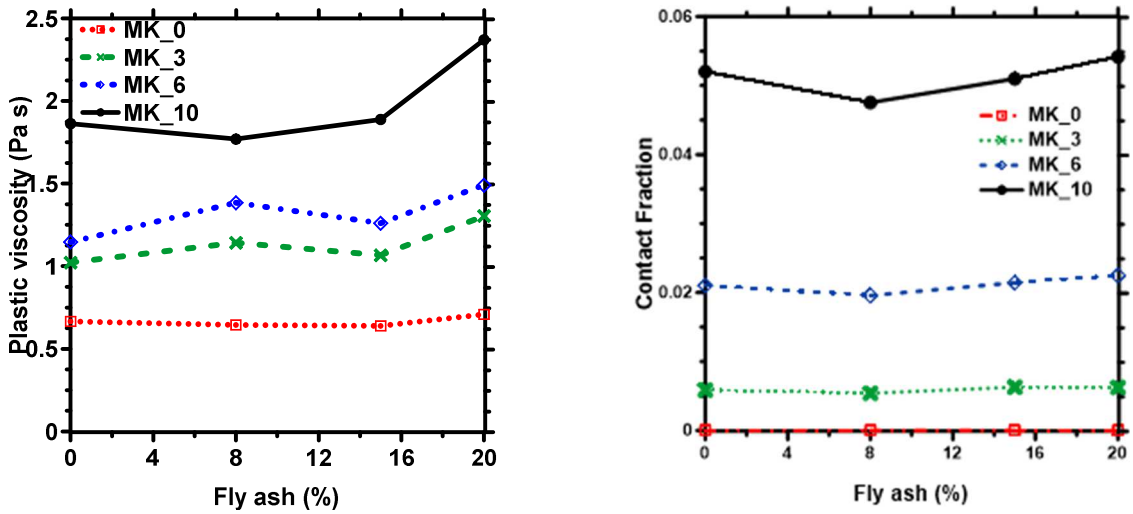

Figure 25: a) Influence of MK-FA on the Plastic Viscosity b) Contact Fraction between MK-FA Particles.

Figure 25 a) illustrates that the plastic viscosity, similar to the yield stress increases with an increase in metakaolin content. At 10% metakaolin an increase of 180% in the plastic viscosity is observed compared to 0% metakaolin plastic viscosity. There is a growth in the plastic viscosity with use of class F fly ash which is an unexpected trend which will be explained in the following paragraph. In higher metakaolin blends there is a comparative more influence of fly ash particles than in lower metakaolin blends inferred from higher plastic viscosity values.

Metakaolin particles as mentioned earlier have a plate like shape and thus have large surface area. The contact fractions between metakaolin particles is very high as seen from the Figure 25 b). This is expected of a material with very small mean particle size (5 microns) and a high specific surface area as can be seen from Table 3. These particles thus have a high friction between them when a shear stress is applied causing resistance to flow and thus a high value of plastic viscosity. Introduction of spherical shaped particles like class F fly ash are usually expected to lower the plastic viscosity of the material, instead a reverse effect is taking place. The increase in viscosity with an increase in the fly ash particles could be attributed to better packing of metakaolin particles with higher fly ash content due to well graded mix which overcomes the effect of low friction particles.

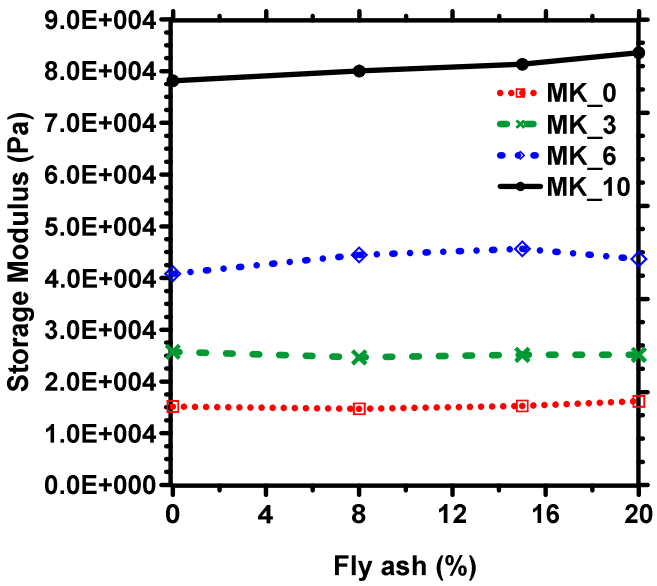

Figure 26: Influence of MK-FA on Storage Modulus.

Storage modulus of the paste was found by applying oscillatory stress to the material. Figure 26 shows the storage modulus results with increment of metakaolin and fly ash. It is observed that an increment in fly ash from 0% to 20% in the paste resulted in an increase in the storage modulus by 6% at various levels of metakaolin. There was a huge increase in G' by 4 times as metakaolin proportion was increased from 0% to 10%.

Storage modulus is mainly influenced by the number solids in the system, as iron is replaced by fly ash particles the solids in the system increase thus increasing the storage modulus. As fly ash particles are lighter and smaller as compared to iron, the same mass of iron when replaced by fly ash occupies more number of particles in the mix. Thus more solid like elastic properties in the system increase.

5.3.2 Effect of Iron on the Rheological Properties.

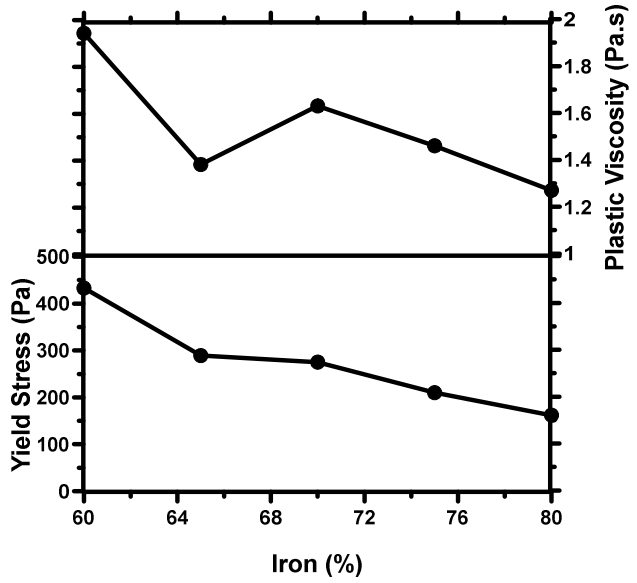

Figure 27: Effect of Iron on Yield Stress and Plastic Viscosity.

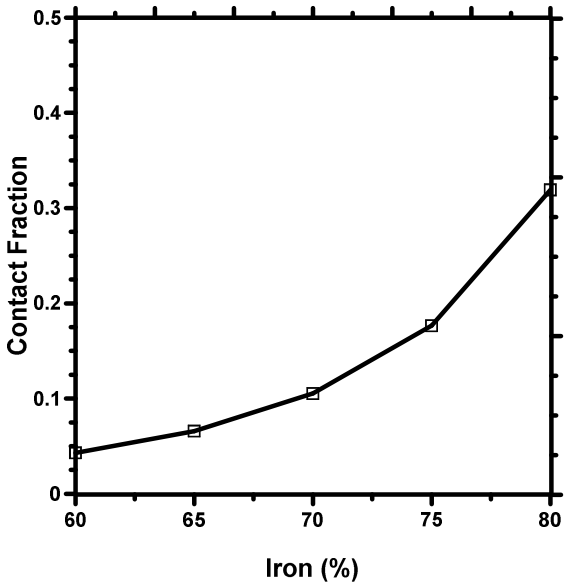

Figure 28: Contact Fraction between Iron Particles.

The yield stress and plastic viscosity can be observed to decrease with an increment in the iron content in the binder in Figure 27. As the iron content is increased from 60% to 80% mass, the yield stress values fall by 60% and plastic viscosity decreases by 35%. There is almost a steady decrease in both the parameters.

This behavior can be explained by using the median particle size. Iron particles which have a mean particle size of 19 micron was added to the mix by replacing same mass of limestone which has a mean particle size of 1.4 micron. Such addition of coarse material in place of fine particles increases the distance between particles and thus the inter-particle spacing. Higher the spacing between particles lower is the force of attraction between them and thus leads to a decrease in yield stress.

An increase in iron content, leads to an increase in the number of iron particles that are in contact with each other. The contact fraction increases with increasing iron content as shown in Figure 28. Plastic viscosity can thus said to be inversely proportional to the contact fraction of iron particles. Iron has a high zeta potential and thus does not coagulate when added to water. There is plenty of water available for mass transfer which causes the plastic viscosity to decrease.

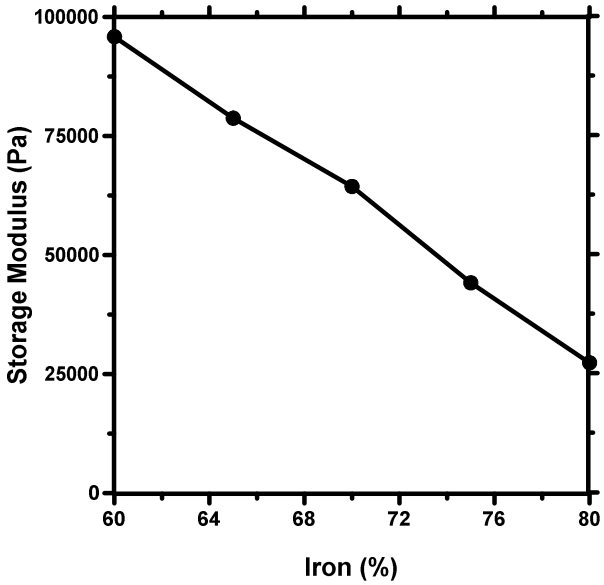

Figure 29: Effect of Iron on Storage Modulus of Iron Binder System.

Figure 29 shows a steady decrease in the storage modulus of the paste by 70%, with an

increase in iron content from 60% to 80%. The explanation for this is similar to the explanation for storage modulus in MK-FA paste. As iron replaces light weight limestone in the system, the volume of solids in the system decrease because iron particles are coarse particles with high specific gravity whereas limestone are fine particles with comparatively lower specific gravity. Such high concentration of coarse particles in the system affects the particle packing and lowers the G' values.

5.4 OPC-iron Binder System.

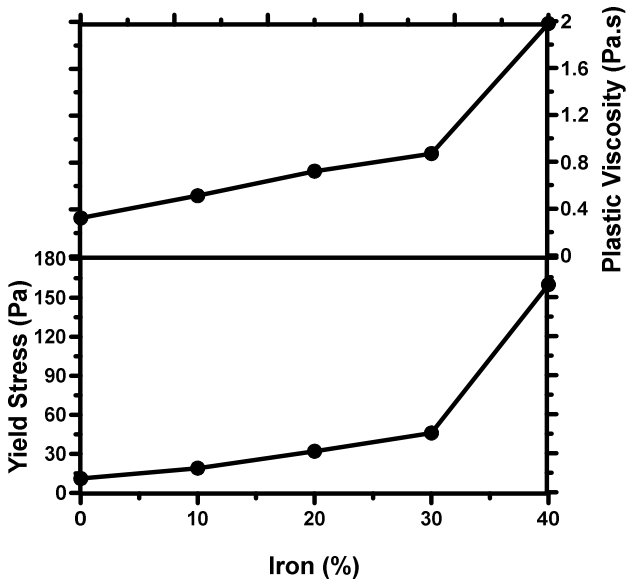

Figure 30: Yield Stress and Plastic Viscosity of OPC-Iron Binder System.

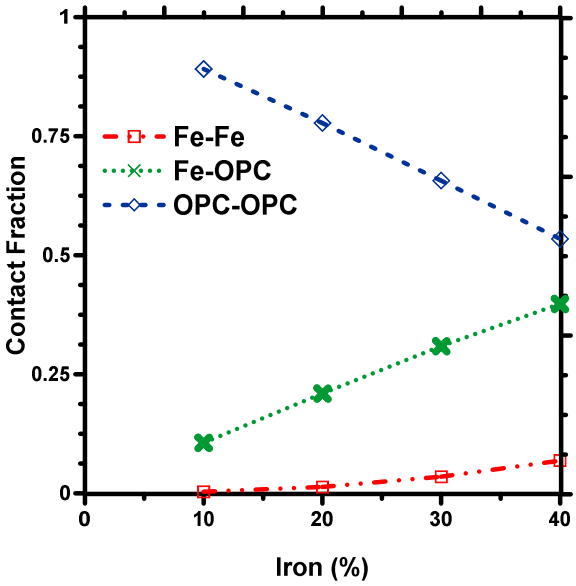

Figure 31: Contact Fraction between Iron, OPC and OPC-Iron Particles.

In the OPC-iron binder system OPC is replaced by iron from 0 to 40%. This replacement resulted in an increase in the yield stress and plastic viscosity from Figure 30. The increase in both the parameters was gradual until 30% replacement, beyond which there was a bump in these values.

As discussed in previous chapter, it is known that OPC has a strong tendency to agglomerate when mixed with water. This is the reason for yield stress in OPC, but when OPC is replaced by iron which does not agglomerate yet the yield stress was seen to increase. The reason for this behavior of the paste is that iron particles act as reinforcements in the OPC matrix. With increasing replacement of OPC by iron the matrix in the system reduces but is enough to hold the iron particles in it until 30 %. As more angular particles are introduced in the form of iron, there is better interlocking and friction between particles. The contact fraction between iron and OPC increases with replacement which means there is better particle size distribution in the system leading to better packing of iron and OPC particles causing a surge in yield stress and plastic viscosity.

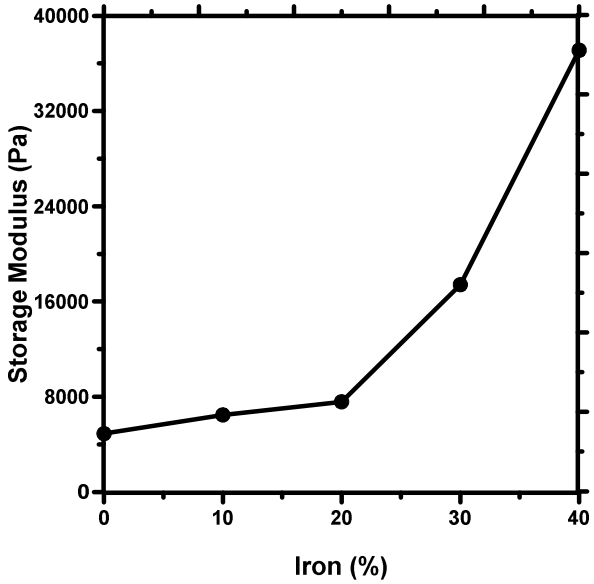

Figure 32: Storage Modulus of OPC-Iron Binder.

The storage modulus of OPC-iron binder system increases with an increase in iron content of the system, as can be seen from Figure 32. The value of G' increases by 6 times with an increase in iron content from 0% to 40%. The figure shows a gradual increase in G' until 20% iron, G' increases exponentially when iron content was increased more than 20% in the mix.

OPC is a cohesive material and agglomerates when water is added to the mix. When an elastic material like iron is introduced in the system, it behaves as a reinforcement and improves the elastic properties of the mix. Beyond 20% replacement the iron particles pack very well with the OPC particles to produce higher G' values. This was also observed during mixing the system with iron content of more than 20%. The paste had very low fluidity compared to low iron content systems.

6 CONCLUSION

6.1 Time Dependent Rheological Response of OPC-SCM Binders with Addition of Superplasticizers.

The main conclusions drawn in the time dependent study of the effect of OPC replacement by SCM are as follows:

- Class C and class F fly ash addition to OPC decreases the yield stress and plastic viscosity of the binary system. This behavior was due to the spherical shape of fly ash particles, electrostatic repulsive force and because these particles are coarser than OPC, which leads to larger inter-particle spacing and lower contact fraction.
- The rate of hydration of the system also slows down as the C_3A and C_3S content in the paste reduces with replacement by fly ash. Production of C-S-H is slower resulting in delayed structure formation which leads to slow growth in yield stress and plastic viscosity.
- The storage modulus decreased with replacement by SCM and increased at a slower rate with time as compared to OPC. The influence of solid loading is found to be the dominating factor on the storage modulus.
- Superplasticizers have a huge influence on the rheological properties until the effect of superplasticizer diminished. They are adsorbed on the surface of C3A and C4AF and make them negatively charged causing a repulsive force between particles thus reducing the yield stress, plastic viscosity and storage modulus.

6.2 Rheological Response of Iron Binder System.

The rheological characterization of composite iron binder brought about explorations of

several key phenomena in these systems:

- Metakaolin have a strong influence on the yield stress, plastic viscosity and storage modulus due to its tendency to agglomerate and retain water. These are very fine particles with huge specific surface area which decrease the inter-particle spacing and increase the mentioned properties.
- Fly ash has comparatively lower influence on the rheological behavior because it does not agglomerate when mixed with water and it contributes marginally due to better grading and particle packing between different mixes because of its spherical shape
- Iron formed a major portion of the iron binder system, thus when further increased from 60% to 80%, the yield stress, plastic viscosity and storage modulus were observed to decrease. This observation can be attributed to the coarse nature of iron powder and its high zeta potential which does not allow the particle to agglomerate.
- In the OPC-iron binder system, an increase in replacement of OPC by iron resulted in an increase in the rheological parameters. This behavior of the system was because the iron particles behaved as reinforcements in the OPC matrix and increased the elastic and viscous nature of the system.

WORK CITED

Arora, Aashay, Gaurav Sant, and Narayanan Neithalath. 2016. "Ternary Blends Containing Slag and Interground/blended Limestone: Hydration, Strength, and Pore Structure." *Construction and Building Materials* 102, Part 1 (January): 113–24. doi:10.1016/j.conbuildmat.2015.10.179.

Asaga, K., and D. M. Roy. 1980. "Rheological Properties of Cement Mixes: IV. Effects of Superplasticizers on Viscosity and Yield Stress." *Cement and Concrete Research* 10 (2): 287–95. doi:10.1016/0008-8846(80)90085-X.

"ASTM C143 - 12. Standard Test Method for Slump of Hydraulic-Cement Concrete." 2012. *ASTM International, West Conshohocken, PA.*

"ASTM C150 / C150M - 12. Standard Specification for Portland Cement." 2012. *ASTM International, West Conshohocken, PA.*

"ASTM C568 / C568M - 10. Standard Specification for Limestone Dimension Stone." 2012. *ASTM International, West Conshohocken, PA.*

Banfill, P. F. G. 2003. "The Rheology of Fresh Cement and Concrete–a Review. 11th Int." *Cem, Chem. Congr. Dublin*.

Barnes, Howard A. 2000. "A Handbook of Elementary Rheology." http://cspcbsr1.swan.ac.uk/innfm_updated/innfmshop/products/FilmFlyer.doc.

Bayod, Elena, Ene Pilman Willers, and Eva Tornberg. 2008. "Rheological and Structural Characterization of Tomato Paste and Its Influence on the Quality of Ketchup." *LWT-Food Science and Technology* 41 (7): 1289–1300.

Bentz, Dale P. 2000. "CEMHYD3D: A Three-Dimensional Cement Hydration and Microstructure Development Modelling Package. Version 2.0." *National Institute of Standards and Technology Interagency Report* 7232. ftp://129.6.13.25/pub/bfrl/bentz/CEMHYD3D/version30/manual/NISTIR7232.pdf .

Bentz, Dale P., Chiara F. Ferraris, Michael A. Galler, Andrew S. Hansen, and John M. Guynn. 2012. "Influence of Particle Size Distributions on Yield Stress and Viscosity of Cement–fly Ash Pastes." *Cement and Concrete Research* 42 (2): 404–9. doi:10.1016/j.cemconres.2011.11.006.

Betioli, A. M., P. J. P. Gleize, D. A. Silva, V. M. John, and R. G. Pileggi. 2009. "Effect of HMEC on the Consolidation of Cement Pastes: Isothermal Calorimetry versus Oscillatory Rheometry." *Cement and Concrete Research* 39 (5): 440–45. doi:10.1016/j.cemconres.2009.02.002.

Bingham, Eugene Cook. 1922. *Fluidity and Plasticity*. Vol. 2. McGraw-Hill Book Compny, Incorporated.

Brooks, J. J, and M. A Megat Johari. 2001. "Effect of Metakaolin on Creep and Shrinkage of Concrete." *Cement and Concrete Composites*, Metakaolin and Calcined Clays, 23 (6): 495–502. doi:10.1016/S0958-9465(00)00095-0.

Burgos-Montes, Olga, Marta Palacios, Patricia Rivilla, and Francisca Puertas. 2012. "Compatibility between Superplasticizer Admixtures and Cements with Mineral Additions." *Construction and Building Materials* 31 (June): 300–309. doi:10.1016/j.conbuildmat.2011.12.092.

Casson, N. 1959. *A Flow Equation for Pigment-Oil Suspensions of the Printing Ink Type*. Vol. 84. Pergamon, London.

Cerny, L. C., F. B. Cook, and C. C. Walker. 1962. "Rheology of Blood." *American Journal of Physiology -- Legacy Content* 202 (6): 1188–94.

Chandra, S., and J. Björnström. 2002. "Influence of Cement and Superplasticizers Type and Dosage on the Fluidity of Cement mortars—Part I." *Cement and Concrete Research* 32 (10): 1605–11. doi:10.1016/S0008-8846(02)00839-6.

Chomton, G., and P. J. Valyer. 1972. "APPLIED RHEOLOGY OF ASPHALT MIXES PRACTICAL APPLICATION." In . Vol. 1. http://trid.trb.org/view.aspx?id=138840.

Das, Sumanta, Ahmet Kizilkanat, and Narayanan Neithalath. 2015. "Crack Propagation and Strain Localization in Metallic Particulate-Reinforced Cementitious Mortars." *Materials & Design* 79 (August): 15–25. doi:10.1016/j.matdes.2015.04.038.

Das, Sumanta, Beshoy Souliman, David Stone, and Narayanan Neithalath. 2014. "Synthesis and Properties of a Novel Structural Binder Utilizing the Chemistry of Iron Carbonation." *ACS Applied Materials & Interfaces* 6 (11): 8295–8304. doi:10.1021/am5011145.

Dhir, R. K., and M. R. Jones. 1999. "Development of Chloride-Resisting Concrete Using Fly Ash." *Fuel* 78 (2): 137–42. doi:10.1016/S0016-2361(98)00149-5.

Dintenfass, Leopold. 1976. *Rheology of Blood in Diagnostic and Preventive Medicine: An Introduction to Clinical Haemorheology*. Butterworths.

Ferraris, Chiara F., Karthik H. Obla, and Russell Hill. 2001. "The Influence of Mineral Admixtures on the Rheology of Cement Paste and Concrete." *Cement and Concrete Research* 31 (2): 245–55.

Frías, M., M. I. Sánchez de Rojas, and J. Cabrera. 2000. "The Effect That the Pozzolanic Reaction of Metakaolin Has on the Heat Evolution in Metakaolin-Cement Mortars." *Cement and Concrete Research* 30 (2): 209–16. doi:10.1016/S0008-8846(99)00231-8.

Gaskins, Frederick H., John G. Brodnyan, Wladimir Philippoff, and Edmund Thelen. 1960. "The Rheology of Asphalt. II. Flow Characteristics of Asphalt." *Transactions of The Society of Rheology (1957-1977)* 4 (1): 265–78.

Gołaszewski, Jacek, and Janusz Szwabowski. 2004. "Influence of Superplasticizers on Rheological Behaviour of Fresh Cement Mortars." *Cement and Concrete Research* 34 (2): 235–48. doi:10.1016/j.cemconres.2003.07.002.

Grzeszczyk, Stefania, and Grzegorz Lipowski. 1997. "Effect of Content and Particle Size Distribution of High-Calcium Fly Ash on the Rheological Properties of Cement Pastes." *Cement and Concrete Research* 27 (6): 907–16. doi:10.1016/S0008-8846(97)00073-2.

Herschel, W. H., and R. Bulkley. 1926. "Measurement of Consistency as Applied to Rubber-Benzene Solutions." In *Am. Soc. Test Proc*, 26:621–33.

Lachemi, M., K. M. A. Hossain, V. Lambros, P.-C. Nkinamubanzi, and N. Bouzoubaa. 2004. "Performance of New Viscosity Modifying Admixtures in Enhancing the Rheological Properties of Cement Paste." *Cement and Concrete Research* 34 (2): 185–93.

Mueller, S., E. W. Llewellin, and H. M. Mader. 2009. "The Rheology of Suspensions of Solid Particles." *Proceedings of the Royal Society of London A: Mathematical, Physical and Engineering Sciences*, December, rspa20090445. doi:10.1098/rspa.2009.0445.

Nehdi, M., and M. -A. Rahman. 2004. "Estimating Rheological Properties of Cement Pastes Using Various Rheological Models for Different Test Geometry, Gap and Surface Friction." *Cement and Concrete Research* 34 (11): 1993–2007. doi:10.1016/j.cemconres.2004.02.020.

Park, C. K., M. H. Noh, and T. H. Park. 2005. "Rheological Properties of Cementitious Materials Containing Mineral Admixtures." *Cement and Concrete Research* 35 (5): 842–49. doi:10.1016/j.cemconres.2004.11.002.

Powers, T. C. 1958. "Structure and Physical Properties of Hardened Portland Cement Paste." *Journal of the American Ceramic Society* 41 (1): 1–6. doi:10.1111/j.1151-2916.1958.tb13494.x.

Roussel, N. 2006. "Correlation between Yield Stress and Slump: Comparison between Numerical Simulations and Concrete Rheometers Results." *Materials and Structures* 39 (4): 501–9. doi:10.1617/s11527-005-9035-2.

Roussel, N., and P. Coussot. 2005. "'Fifty-Cent Rheometer' for Yield Stress Measurements: From Slump to Spreading Flow." *Journal of Rheology (1978-Present)* 49 (3): 705–18. doi:10.1122/1.1879041.

Röβler, M., and I. Odler. 1985. "Investigations on the Relationship between Porosity, Structure and Strength of Hydrated Portland Cement Pastes I. Effect of Porosity." *Cement and Concrete Research* 15 (2): 320–30. doi:10.1016/0008-8846(85)90044-4.

Saak, Aaron W., Hamlin M. Jennings, and Surendra P. Shah. 2001. "The Influence of Wall Slip on Yield Stress and Viscoelastic Measurements of Cement Paste." *Cement and Concrete Research* 31 (2): 205–12. doi:10.1016/S0008-8846(00)00440-3.

Sakai, Etsuo, Keisuke Masuda, Yasuo Kakinuma, and Yutaka Aikawa. 2009. "Effects of Shape and Packing Density of Powder Particles on the Fluidity of Cement Pastes with Limestone Powder." *Journal of Advanced Concrete Technology* 7 (3): 347–54. doi:10.3151/jact.7.347.

Siddique, Rafat, and Juvas Klaus. 2009. "Influence of Metakaolin on the Properties of Mortar and Concrete: A Review." *Applied Clay Science* 43 (3–4): 392–400. doi:10.1016/j.clay.2008.11.007.

Steffe, James Freeman. 1996. *Rheological Methods in Food Process Engineering*. Freeman press.

Subramaniam, Kolluru V., and Xiaojun Wang. 2010. "An Investigation of Microstructure Evolution in Cement Paste through Setting Using Ultrasonic and Rheological Measurements." *Cement and Concrete Research* 40 (1): 33–44. doi:10.1016/j.cemconres.2009.09.018.

Sun, Zhihui, Thomas Voigt, and Surendra P. Shah. 2006. "Rheometric and Ultrasonic Investigations of Viscoelastic Properties of Fresh Portland Cement Pastes." *Cement and Concrete Research* 36 (2): 278–87. doi:10.1016/j.cemconres.2005.08.007.

Vance, Kirk, Aditya Kumar, Gaurav Sant, and Narayanan Neithalath. 2013. "The Rheological Properties of Ternary Binders Containing Portland Cement, Limestone, and Metakaolin or Fly Ash." *Cement and Concrete Research* 52 (October): 196–207. doi:10.1016/j.cemconres.2013.07.007.

Vance, Kirk, Gaurav Sant, and Narayanan Neithalath. 2015. "The Rheology of Cementitious Suspensions: A Closer Look at Experimental Parameters and Property Determination Using Common Rheological Models." *Cement and Concrete Composites* 59 (May): 38–48. doi:10.1016/j.cemconcomp.2015.03.001.

Voigt, Thomas, Guang Ye, Zhihui Sun, Surendra P. Shah, and Klaas van Breugel. 2005. "Early Age Microstructure of Portland Cement Mortar Investigated by Ultrasonic Shear Waves and Numerical Simulation." *Cement and Concrete Research* 35 (5): 858–66. doi:10.1016/j.cemconres.2004.09.004.